

Summarizing Bayesian Nonparametric Mixture Posterior - Sliced Optimal Transport Metrics for Gaussian Mixtures

Khai Nguyen

Department of Statistics and Data Sciences, University of Texas at Austin
and

Peter Mueller

Department of Mathematics, University of Texas at Austin

May 9, 2025

Abstract

Existing methods to summarize posterior inference for mixture models focus on identifying a point estimate of the implied random partition for clustering, with density estimation as a secondary goal (Wade and Ghahramani, 2018; Dahl et al., 2022). We propose a novel approach for summarizing posterior inference in nonparametric Bayesian mixture models, prioritizing estimation of the mixing measure (or mixture) as an inference target. One of the key features is the model-agnostic nature of the approach, which remains valid under arbitrarily complex dependence structures in the underlying sampling model. Using a decision-theoretic framework, our method identifies a point estimate by minimizing posterior expected loss. A loss function is defined as a discrepancy between mixing measures. Estimating the mixing measure implies inference on the mixture density and the random partition. Exploiting the discrete nature of the mixing measure, we use a version of sliced Wasserstein distance. We introduce two specific variants for Gaussian mixtures. The first, mixed sliced Wasserstein, applies generalized geodesic projections on the product of the Euclidean space and the manifold of symmetric positive definite matrices. The second, sliced mixture Wasserstein, leverages the linearity of Gaussian mixture measures for efficient projection¹.

Keywords: Random partition models; Density estimation; Cluster estimation.

¹The code for the paper is published at <https://github.com/khainb/sbnpm-sot>.

1 Introduction

We propose an approach to summarize the posterior distribution on the random mixing measure in Bayesian nonparametric (BNP) mixture models (Ghosal and van der Vaart, 2017). By focusing on the mixing measure, the method fills a gap in the existing literature which focuses on summarizing the posterior distribution of implied random partitions of experimental units (Wade and Ghahramani, 2018; Dahl et al., 2022). The proposed approach requires only posterior Monte Carlo samples of random mixing measures as input and provides a well-defined summary of these measures. The approach is valid with any posterior simulation method. Importantly, the approach is model-agnostic, accommodating any prior distributions on the random mixing measures, including those with dependent structures such as dependent Dirichlet process (Quintana et al., 2022; MacEachern, 1999). Using the resulting point estimate of the mixing measure, if desired, one can derive an estimate of the density function and the partition.

Most approaches to posterior summarization for BNP mixture models assume a context of density estimation, conditioning on a sample $\{Y_1, \dots, Y_n\}$ from a mixture. Latent indicators z_i , $i = 1, \dots, n$ that link the data with atoms in the mixing measure define a random partition $\rho = \{S_1, \dots, S_K\}$ of $[n] := \{1, \dots, n\}$ into subsets S_k of matching z_i . Methods then aim to summarize $p(\rho \mid Y_1, \dots, Y_n)$, or equivalently, $p(\mathbf{z} \mid Y_1, \dots, Y_n)$ for $\mathbf{z} = (z_1, \dots, z_n)$.

Proceeding under a decision-theoretic framework involves minimizing the posterior expectation of a chosen loss function to define the Bayes rule:

$$\hat{\rho}^* = \arg \min_{\hat{\rho}} \mathbb{E}[\mathcal{L}(\rho, \hat{\rho}) \mid Y_1, \dots, Y_n] \quad \text{or} \quad \hat{\mathbf{z}}^* = \arg \min_{\hat{\mathbf{z}}} \mathbb{E}[\mathcal{L}(\mathbf{z}, \hat{\mathbf{z}}) \mid Y_1, \dots, Y_n], \quad (1)$$

where \mathcal{L} is a loss function that can be expressed using both the partition or the cluster label notation. Lau and Green (2007) propose the use of Binder loss (Binder, 1978).

Wade and Ghahramani (2018) use variational information (VI) loss (Meilă, 2007) as an alternative. Other information-based distances include normalized variational information (NVI), information distance (ID), normalized information distance (NID) (Nguyen et al., 2010), one minus adjusted Rand index (omARI) (Rand, 1971), generalized Binder and VI (Dahl et al., 2022). In addition to selecting the loss function, various search algorithms have been proposed to solve the optimization problem in (1), including binary integer programming (Lau and Green, 2007), greedy search based on the Hasse diagram (Wade and Ghahramani, 2018), the R & F algorithm (Rastelli and Friel, 2018), and the SALSO algorithm (Dahl et al., 2022).

Even when the primary inference target is a posterior summary of ρ , estimation of the mixture or the mixing measure can still be reported in a second step via additional sampling. Also, in many cases it is convenient to focus on the mixing measure since the mixing measure implies both the partition and the density. Moreover, summarizing the mixing measure can avoid dealing with label switching problems that arises when summarizing the partition. Consider then a general BNP mixture model: $Y_1, \dots, Y_n \stackrel{i.i.d.}{\sim} F$, $F = f * G$, $G \sim p(G)$, where f is a kernel, $*$ denotes the convolution operator, F is the mixture density, and G is the mixing measure (or the mixture). We propose to find a summary for $p(G|Y_1, \dots, Y_n)$. From a point estimate \hat{G} , one can directly obtain a point estimate of the density \hat{F} as a convolution with the density kernel f . And if desired, one can obtain a point estimate $\hat{\rho}$ (or cluster labels \hat{z}) induced by \hat{G} . For the sake of easy exposition, in the upcoming discussion we assume i.i.d. sampling. But we do so without loss of generality. The only assumption is that posterior inference is provided as a posterior Monte Carlo sample of G . The details of the sampling model, prior model, and the details of the posterior Monte Carlo simulation scheme can be arbitrary.

Similar to (1), we continue to use a decision-theoretic approach by minimizing a posterior expected loss. However, targeting G , we require a loss function that quantifies discrep-

ancy between two measures. Given the discrete nature of the random measure G , optimal transport distances (Villani, 2009; Peyré et al., 2019) are a natural choice in this context. Specifically, we choose sliced Wasserstein (SW) distance (Rabin et al., 2012; Bonneel et al., 2015) due to its computational and statistical scalability with respect to the number of dimensions and the number of support points. With near-linear time complexity in the number of support points, the SW distance facilitates efficient and accurate truncation of mixing measures.

Recall that our primary inference aim is summarizing the mixing measure. If the primary goal were the mixture density, a more natural option would be to work with less parsimonious, but easier tractable location mixtures. Considering general mixture of Gaussians, we introduce two novel versions of SW, working with measures supported on the product of the Euclidean manifold and the manifold of symmetric positive definite (SPD) matrices. The first variant, called mixed SW (Mix-SW), uses generalized geodesic projection instead of the conventional linear projection used in standard SW. Consequently, Mix-SW preserves more geometric information compared to SW with a vectorization approach. The second variant, named sliced mixture Wasserstein (SMix-W), compares mixing measures by evaluating the induced mixture of Gaussian measures. By leveraging the linearity properties of mixture of Gaussian measures, SMix-W achieves a reduction in projection complexity compared to traditional SW while still being geometrically meaningful. Finally, we discuss basic properties of the proposed distances including boundedness and metricity.

The remainder of the article is organized as follows: In Section 2, we introduce the approach for summarizing the posterior of random mixing measures. Section 3 presents the two novel distances for Gaussian mixing measures, accompanied by a discussion of their theoretical and computational properties. In Section 4, we conduct an empirical analysis using simulated data and the Old Faithful Geyser dataset, employing a truncated Dirichlet Process Gaussian mixture model. We assess the proposed approach in both clustering and

density estimation. Additional materials, including technical proofs, are provided in the appendices. We refer the reader to Appendix A.1 for the list of acronyms in the paper.

2 Point estimation of random mixing measures

We present a new approach for obtaining a point estimate of random mixing measures. Without loss of generality we consider the setting of inference under following BNP mixture model: $Y_1, \dots, Y_n \stackrel{\text{i.i.d.}}{\sim} F$, $F = f * G$, $G \sim p(G)$, where f is a kernel and $p(G)$ denotes a prior on the random mixing measure G . Our objective is to report a point estimate \hat{G} . The point estimate can then be used for any downstream data analysis. We first define the problem in Section 2.1 and then discuss current options for optimal transport distances that can be used as the loss function in Section 2.2.

2.1 Problem Setup

Let Θ denote the space of supports of the mixing measure G . Under a decision-theoretic framework, the point estimate of the mixing measure \hat{G}^* minimizes posterior expected loss:

$$\hat{G}^* = \arg \min_{\hat{G}} \mathbb{E}[\mathcal{D}(G, \hat{G}) \mid Y_1, \dots, Y_n], \quad (2)$$

where $\mathcal{D} : \mathcal{P}(\Theta) \times \mathcal{P}(\Theta) \rightarrow \mathbb{R}_+$ can be chosen as a distance on the space of measures supported on Θ . Since the posterior is usually intractable, the expectation in (2) is approximated using posterior samples generated by Monte Carlo methods such as Markov chain Monte Carlo (MCMC) posterior simulation. Given M posterior Monte Carlo samples, $G_1, \dots, G_M \sim p(G \mid Y_1, \dots, Y_n)$, the optimization problem can be approximated as

$$\hat{G}^* = \arg \min_{\hat{G}} \frac{1}{M} \sum_{m=1}^M \mathcal{D}(G_m, \hat{G}). \quad (3)$$

We use a simple greedy procedure to solve the optimization problem in (3). Specifically, we construct an $M \times M$ matrix, where the entry in row i and column j represents the distance $\mathcal{D}(G_i, G_j)$ between the i -th and j -th posterior samples. We then identify the index i^* that minimizes the average distance across columns, $\frac{1}{M} \sum_{j=1}^M \mathcal{D}(G_i, G_j)$, and return G_{i^*} as the greedy solution. This is equivalent to selecting the best posterior sample from the posterior Monte Carlo samples. We give a pseudo algorithm to describe the procedure in Algorithm 1 in Appendix A.5.

In practice, truncating the mixing measure G can accelerate computation, improve convergence and simplify implementation (Ishwaran and James, 2001). Specifically, we can use the following truncated version of G : $\bar{G} = \sum_{k=1}^K \alpha_k \delta_{\theta_k}$ with $0 < K < \infty$. From Theorem 1 in Ishwaran and James (2001), we can choose the truncation level based on the moments of the random weights. For example, under a Dirichlet process prior on G , we can choose K such that $(\alpha_0/(\alpha_0 + 1))^{K-1}$ is small enough (α_0 is the concentration parameter). Ideally, we want to choose the largest feasible value of K to minimize the approximation error introduced by truncation. We then approximate the distance between two measures by the distance between the truncated versions, i.e., $\mathcal{D}(G_1, G_2) \approx \mathcal{D}(\bar{G}_1, \bar{G}_2)$. Alternatively, one could proceed with random truncation as discussed in Griffin (2016) or use a slice sampler (Kalli et al., 2011). Any alternative method could be used, as long as it provides a posterior Monte Carlo sample of the mixing measure. Moreover, the proposed approach does not require matching truncation levels across Monte Carlo samples. Under marginal MCMC (Neal, 2000), the algorithm can proceed with the empirical distribution of an imputed sample from G . Under a marginal algorithm, the latter can be generated.

A point estimate of the mixing measure \hat{G} , implies a point estimate of the density by convolution with the kernel as $\hat{F} = f * \hat{G}$. To estimate the partition, we determine the

cluster membership indicator z_i by maximum a posteriori (MAP):

$$\hat{z}_i = \arg \max_{k \in \{1, \dots, K\}} p(z_i = k \mid \hat{G}, y_i). \quad (4)$$

Here y_i generically denotes an observed data point. Under the point estimate of the truncated mixing measure, i.e., $\hat{G} \approx \sum_{k=1}^K \hat{w}_k \delta_{\hat{\theta}_k}$, this becomes:

$$\hat{z}_i = \arg \max_{k \in \{1, \dots, K\}} p(z_i = k \mid \hat{w}_1, \dots, \hat{w}_K, \hat{\theta}_1, \dots, \hat{\theta}_K, y_i). \quad (5)$$

While there are alternative methods to obtain a point estimate \hat{z} given the mixing measure such as sampling or using a decision theoretic framework with Monte Carlo samples from $p(z_i \mid \hat{w}_1, \dots, \hat{w}_K, \hat{\theta}_1, \dots, \hat{\theta}_K, y_i)$, we prefer the MAP as a natural and computationally efficient approach. In addition, it is possible to extend the framework to summarize the density F directly. However, such an approach would not be computationally efficient since it might require evaluating the density on a grid of exponentially increasing size with increasing dimension. Moreover, obtaining a point estimate of the random partition would become complicated.

In the optimization in (3), after truncation, we require distances for pairs of discrete mixing measures that may have disjoint supports. Traditional f -divergences (Ali and Silvey, 1966), such as the Kullback–Leibler (KL) divergence, Jensen–Shannon (JS) divergence, and others, cannot directly be used because they require access to the density ratio, which may be undefined in this context. Consequently, optimal transport (OT) metrics become a natural choice in this scenario. We will briefly discuss currently available OT distances.

2.2 Optimal Transport Distances for the loss function

Let $G_1, G_2 \in \mathcal{P}(\Theta)$ and $c : \Theta \times \Theta \rightarrow \mathbb{R}^+$ be a ground metric. The Wasserstein- p ($p \geq 1$) distance (Villani, 2009) between two measures G_1 and G_2 is defined as follows:

$$W_c^p(G_1, G_2) = \inf_{\pi \in \Pi(G_1, G_2)} \int_{\Theta \times \Theta} c(x, y)^p d\pi(x, y), \quad (6)$$

where $\Pi(G_1, G_2) = \{\pi \in \mathcal{P}(\Theta \times \Theta) \mid \pi(A, \Theta) = G_1(A), \pi(\Theta, B) = G_2(B) \forall A, B \subset \Theta\}$ is the set of all transportation plans/couplings. When G_1 and G_2 are discrete measures, i.e., $G_1 = \sum_{i=1}^{K_1} \alpha_i \delta_{x_i}$ and $G_2 = \sum_{j=1}^{K_2} \beta_j \delta_{y_j}$, the Wasserstein distance can be rewritten as:

$$W_c^p(G_1, G_2) = \min_{\pi \in \Gamma(\alpha, \beta)} \sum_{i=1}^{K_1} \sum_{j=1}^{K_2} c(x_i, y_j)^p \pi_{ij}, \quad (7)$$

where the set of transportation plans becomes $\Gamma(\alpha, \beta) = \{\pi \in \mathbb{R}_+^{K_1 \times K_2} \mid \pi \mathbf{1} = \beta, \pi^\top \mathbf{1} = \alpha\}$. In other words, Wasserstein distance is defined by selecting a coupling/copula π that links the two marginal distributions. Each possible copula is scored by an implied cost of moving probability masses between the atoms/supports of the two discrete measures. Wasserstein distance is then the cost under the optimal, minimum cost copula. The computation of Wasserstein distance is often performed using linear programming (Peyré et al., 2019), with a time complexity of $\mathcal{O}((K_1 + K_2)^3 \log(K_1 + K_2))$. Alternatively, it can be approximated using the entropic regularization approach (Cuturi, 2013), which has a time complexity of $\mathcal{O}(K_1 K_2 \log(K_1 + K_2)/\epsilon)$, where $\epsilon > 0$ is the precision level. Consequently, using Wasserstein distance becomes impractical for large values of K_1 or K_2 . There is one important exception: Wasserstein distance is straightforward in closed-form for univariate measures. This motivates the next construction. When the ground metric $c = \|x - y\|_p$ ($p \geq 1$) is used, we denote $W_c^p(G_1, G_2)$ as $W_p^p(G_1, G_2)$.

SW distance exploits the availability of a closed-form expression for Wasserstein distance on the real line. Specifically, for two distributions $G_1, G_2 \in \mathcal{P}(\mathbb{R})$, the Wasserstein- p

distance is expressed as (Peyré et al., 2019):

$$W_p^p(G_1, G_2) = \int_0^1 |\text{CDF}_{G_1}^{-1}(t) - \text{CDF}_{G_2}^{-1}(t)|^p dt, \quad (8)$$

where $\text{CDF}_{G_1}^{-1}$ denotes the inverse cumulative distribution functions (quantile functions) of G_1 . When $G_1 = \sum_{i=1}^{K_1} \alpha_i \delta_{x_i}$ and $G_2 = \sum_{j=1}^{K_2} \beta_j \delta_{y_j}$ are discrete and assuming that the atoms of the two measures are sorted, the inverse CDFs can be evaluated as

$$\text{CDF}_{G_1}^{-1}(t) = \sum_{i=1}^{K_1} x_i I \left(\sum_{j=1}^{i-1} \alpha_j \leq t \leq \sum_{j=1}^i \alpha_j \right), \quad \text{CDF}_{G_2}^{-1}(t) = \sum_{j=1}^{K_2} y_j I \left(\sum_{i=1}^{j-1} \beta_i \leq t \leq \sum_{i=1}^j \beta_i \right)$$

Solving (8) in this case has the time complexity of $\mathcal{O}((K_1 + K_2) \log(K_1 + K_2))$.

To leverage the closed-form solution of one-dimensional Wasserstein distance in high-dimensional settings, SW distance (Bonneel et al., 2015) is introduced. The central idea of SW is to randomly project two original measures onto one-dimensional measures and then compute the expected value of the one-dimensional Wasserstein distance between the two projected measures. Conventional SW ($\Theta = \mathbb{R}^d$) employs a linear projection, defined as $P_v(x) = \langle v, x \rangle$ for $v \in \mathbb{S}^{d-1}$, where v represents the projection direction. The sliced Wasserstein- p distance ($p \geq 1$) between G_1 and G_2 , using the ground metric $c(x, y) = |x - y|$, is defined as follows:

$$SW_p^p(G_1, G_2) = \mathbb{E}_{v \sim \mathcal{U}(\mathbb{S}^{d-1})} [W_p^p(P_v \# G_1, P_v \# G_2)], \quad (9)$$

where $P_v \# G_1$ and $P_v \# G_2$ are the push-forward measures of G_1 and G_2 through the function P_v , and $\mathcal{U}(\mathbb{S}^{d-1})$ denotes the uniform distribution over the unit hypersphere. For the definition of push-forward measure, given two measurable spaces $(\Theta_1, \mathcal{X}_1)$ and $(\Theta_2, \mathcal{X}_2)$, a measurable function $f : \Theta_1 \rightarrow \Theta_2$, and a measure $G : \mathcal{X}_1 \rightarrow [0, \infty)$, the pushforward of G through f is $f \# G(B) = G(f^{-1}(B))$ for any $B \in \mathcal{X}_2$. In the discrete setting with

$G_1 = \sum_{i=1}^{K_1} \alpha_i \delta_{\theta_i}$, $P_v \# G_1 = \sum_{i=1}^{K_1} \alpha_i \delta_{P_v(\theta_i)}$. Eq (9) formalizes the expectation with respect to the projection P_v of the univariate Wasserstein distances.

The expectation in SW distance is intractable, thus Monte Carlo estimation is often employed to approximate SW. Specifically, let $v_1, \dots, v_L \stackrel{i.i.d.}{\sim} \mathcal{U}(\mathbb{S}^{d-1})$ represent the projecting directions. The Monte Carlo estimation of SW is given by:

$$\widehat{SW}_p^p(G_1, G_2) = \frac{1}{L} \sum_{l=1}^L W_p^p(P_{v_l} \# G_1, P_{v_l} \# G_2). \quad (10)$$

The overall time complexity of SW evaluation is composed of the time required for sampling projecting directions, the time for applying the projection operator P_v , and the time for computing one-dimensional Wasserstein distances. When G_1 and G_2 are discrete measures supported by K_1 and K_2 atoms, respectively, and L Monte Carlo samples are used, the time complexity of SW is: $\mathcal{O}(Ld + Ld(K_1 + K_2) + L(K_1 + K_2) \log(K_1 + K_2)) = \mathcal{O}(Ld(K_1 + K_2) + L(K_1 + K_2) \log(K_1 + K_2))$, where $\mathcal{O}(Ld)$ accounts for sampling projecting directions, $\mathcal{O}(Ld(K_1 + K_2))$ is for the projection, and $\mathcal{O}(L(K_1 + K_2) \log(K_1 + K_2))$ is for computing L one-dimensional Wasserstein distances. Additionally, the projection complexity of SW is $\mathcal{O}(Ld)$, which corresponds to the memory required for storing the L projecting directions. In summary, SW is very scalable in terms of K_1 and K_2 , having i.e., it has near linear complexity in terms of K_1 and K_2 . It allows accurate truncation with large K_1 and K_2 .

A potentially interesting alternative to SW is the multivariate Cramer distance (Baringshaus and Franz, 2004, 2010). Despite being more scalable than Wasserstein distance, it is not as geometrically meaningful since it does not involve finding the optimal coupling between two measures. Moreover, by using entropic regularization, the Wasserstein distance can be seen as a generalization of Cramer distance by forcing the coupling to be an independent coupling (Feydy et al., 2019). In addition, Cramer distance is not as scalable as SW. Cramer distance has quadratic complexity with respect to K_1 and K_2 , while SW has near-linear complexity. Furthermore, SW is also statistically scalable in dimension.

In particular, from Nadjahi et al. (2020); Nguyen et al. (2021); Boedihardjo (2025), we have that $\mathbb{E} \left[\left| SW_p(\hat{G}_{1,K_1}, \hat{G}_{2,K_2}) - SW_p(G_1, G_2) \right| \right] = \mathcal{O}(K_1^{-1/2} + K_2^{-1/2})$ (no exponential relationship between sample size and dimension) for $G_1, G_2 \in \mathcal{P}_p(\mathbb{R}^d)$, where $\hat{G}_{1,K_1}, \hat{G}_{2,K_2}$ are empirical distributions over K_1 and K_2 i.i.d. samples from G_1 and G_2 , respectively. Overall, SW is an attractive option in terms of computational benefits.

3 Sliced Optimal Transport Distances for Gaussian Mixing Measures

For the mixing measures G_1 and G_2 in mixtures of Gaussians, we use parameter space $\Theta = \mathbb{R}^d \times S_d^{++}(\mathbb{R})$, where $S_d^{++}(\mathbb{R})$ is the manifold of all symmetric positive definite matrices. Conventional SW distance can not directly be applied in this context, as it is defined for measures on vector spaces. We first discuss an approach to apply SW using vectorization in Section 3.1. We then propose two novel variants of SW that preserve geometry. In Section 3.2 we start with a new variant of SW based on generalized geodesic projection onto the product of manifolds, which we call Mixed SW (Mix-SW). Finally, we introduce another variant of SW for finite Gaussian mixing measures by comparing their induced mixture measures, which we call sliced mixture Wasserstein (SMix-W). Finally, we note again that in case of a focus on the implied density only, restriction to (less parsimonious, but still flexible) location mixtures is a viable alternative.

3.1 Vectorized Sliced Wasserstein

We are aiming to compare measures on the product of the Euclidean manifold and the manifold of symmetric positive definite (SPD) matrices, denoted as $\Theta = \mathbb{R}^d \times S_d^{++}(\mathbb{R})$, using the SW distance. However, SW is defined on vector spaces. A straightforward approach is to convert measures on $\mathbb{R}^d \times S_d^{++}(\mathbb{R})$ into measures on a vector space. For any

$\theta = (\mu, \Sigma) \in \mathbb{R}^d \times S_d^{++}(\mathbb{R})$, we can arrange the entries of Σ to obtain a vector representation, which can then be stacked with μ . For simplicity, we define the transformation $V(\theta) = (\mu, \Sigma^{(1)}, \dots, \Sigma^{(d)})$, where $\Sigma^{(i)}$ is the i -th row of the matrix Σ . With this transformation, we can redefine SW distance as

$$SW_p^p(G_1, G_2) = \mathbb{E}_{v \sim \mathcal{U}(\mathbb{S}^{d(d+1)-1})}[W_p^p(P_v \# V \# G_1, P_v \# V \# G_2)], \quad (11)$$

for any $G_1, G_2 \in \mathcal{P}(\mathbb{R}^d \times S_d^{++}(\mathbb{R}))$. Despite the attractive simplicity of this approach, there are two main complications to consider. The first is that vectorization destroys the geometry of the space, which may result in a distance that lacks geometric meaning. In contrast to the Wasserstein distance, where the ground metric can be flexibly designed, the ground metric in SW is constrained to exist in a one-dimensional space. The second issue pertains to the high-dimensional projection direction space, $\mathbb{S}^{d(d+1)-1}$, which may require increased computation and memory to achieve accurate approximations via Monte Carlo estimation. The time complexity of vectorized SW is given by $\mathcal{O}(Ld^2(K_1 + K_2) + L(K_1 + K_2) \log(K_1 + K_2))$ and the projection complexity is $\mathcal{O}(Ld^2)$, both of which are quadratic in dimensions. Alternatively, we can also utilize the transformation $V(\theta) = (\mu, B)$ with B as the vectorized version of the upper or lower half of Σ or any triangular factorization. However, the complexity still remains at least quadratic in terms of dimensions. It is worth noting that the vectorization transformation is generic in the sense that it can work with other spaces without a symmetric structure. We present a pseudo algorithm for the vectorization approach in Algorithm 2 in Appendix A.5.

3.2 Mixed Sliced Wasserstein

To address the loss of geometric information, we propose a new variant of SW distance using geodesic projection of the product manifolds $\mathbb{R}^d \times S_d^{++}(\mathbb{R})$. In brief, we define a notion of projecting a support point $(\mu, \Sigma) \in \mathbb{R}^d \times S_d^{++}(\mathbb{R})$ onto a curve with associated velocity vector

$V_w = (w_1v, w_2A)$ (v and A are unit vectors in an appropriate sense which will be defined later) in a way that the projection is easy to evaluate. Using the projection, the desired SW is defined as the expectation of the projected one-dimensional Wasserstein distance, taking the expectation with under the uniform-law over the random curve parameters (v, A, w) .

We begin by reviewing some basic definitions relevant to Riemannian manifolds, including the inner product, geodesics, length, geodesic distance, and the exponential map, as detailed in Appendix A.2. And, we review the concept of geodesic projection (Bonet et al., 2025) and explore certain properties of the manifold of symmetric positive definite matrices $S_d^{++}(\mathbb{R})$ (Pennec et al., 2019) in Appendix A.3.

The geodesic projection and the corresponding SW distance for measures on $S_d^{++}(\mathbb{R})$ have been investigated in Bonet et al. (2023). While the geodesic projection for the product of manifolds was introduced in Bonet et al. (2025), it has not been explicitly derived for any specific case. In this work, we extend the notion of geodesic projection to a generalized geodesic projection by projecting onto a generalized curve with adjusted velocity vectors for each marginal manifold. This adjustment is essential for achieving the identity of indiscernibles (see Appendix A.8) in the subsequently defined SW metric.

Definition 1. *Given a product manifolds $\mathcal{M}_1 \times \mathcal{M}_2$ with the origin $o = (o_1, o_2)$, a generalized curve passing through the origin with the velocity vector $V_w = (w_1v_1, w_2v_2)$ with $\langle v_1, v_1 \rangle_{o_1} = 1$, $\langle v_2, v_2 \rangle_{o_2} = 1$, and $w_1^2 + w_2^2 = 1$, the generalized geodesic projection onto the generalized curve created by V_w is defined as:*

$$P_{V_w}(x) = \arg \min_{t \in \mathbb{R}} c(x, \exp_o(tV_w)), \quad (12)$$

where c is a geodesic distance on the product manifold.

We illustrate the intuition of the generalized geodesic projection in Figure 1. Note that the generalized geodesic projection in (12) is defined as the length ($\arg \min_t$) of the curve

from the origin to the closest point on the curve from x . The generalized geodesic projection has a closed-form expression on $\mathbb{R}^d \times S_d^{++}(\mathbb{R})$ as in the following proposition:

Proposition 1. *The generalized geodesic projection onto a generalized curve passing through the origin with the velocity vector $V_w = (w_1 v, w_2 A)$ ($\|v\|_2^2 = 1, A \in S_d(\mathbb{R}), \|A\|_F^2 = 1, w_1^2 + w_2^2 = 1$) on the product manifold of $\mathbb{R}^d \times S_d^{++}(\mathbb{R})$ has the following form:*

$$P_{V_w}((\mu, \Sigma)) = w_1 \langle \mu, v \rangle + w_2 \text{Trace}(A \log \Sigma).$$

The proof of Proposition 1 is given in Appendix A.6. The generalized geodesic projection (the green diamond in Figure 1) is a weighted combination of the geodesic projection on the Euclidean manifold and the geodesic projection on the manifold $S_d^{++}(\mathbb{R})$. Using the generalized geodesic projection, we now define the mixed Sliced Wasserstein (Mix-SW) distance.

Definition 2. *Given two measures G_1 and G_2 in $\mathcal{P}(\mathbb{R}^d \times S_d^{++}(\mathbb{R}))$, $p \geq 1$, the Mixed Sliced Wasserstein distance is defined as follows:*

$$\text{Mix-SW}_p^p(G_1, G_2) = \mathbb{E}_{(w,v,A) \sim \mathcal{U}(\mathbb{S}) \otimes \mathcal{U}(\mathbb{S}^{d-1}) \otimes \mathcal{U}(S_d(\mathbb{R}))} [W_p^p(P_{V_w} \# G_1, P_{V_w} \# G_2)], \quad (13)$$

where $V_w = (w_1 v, w_2 A)$ and $\mathcal{U}(\mathcal{X})$ is the uniform distribution over the set \mathcal{X} .

Recall that P_{V_w} was defined as a length (on the curve) in (12) implying W_p^p in (13) as distance. Mix-SW is similar to hierarchical hybrid sliced Wasserstein (H2SW) (Nguyen and Ho, 2024). Both definitions combine projections from marginals. However, Mix-SW comes from generalized geodesic projection for a specific product of manifold while H2SW arises from randomly combining two general types of Radon transforms. Also, H2SW is only introduced for the product of the Euclidean manifold and the hypersphere. We first show that $\text{Mix-SW}_p^p(G_1, G_2)$ is bounded as long as the expected geodesic distances with respect to G_1 and G_2 to any point (μ_0, Σ_0) are bounded.

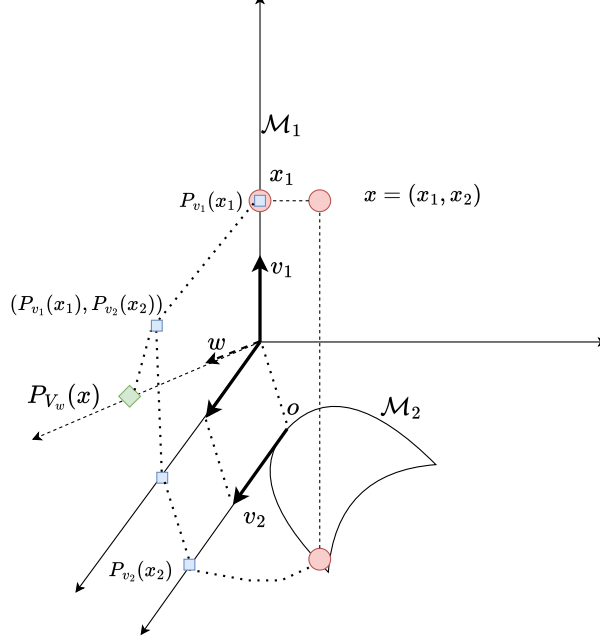


Figure 1: The figure illustrates the computation of generalized geodesic projection of $x = (x_1, x_2)$ (red ball) in $\mathcal{M}_1 \times \mathcal{M}_2$ (\mathcal{M}_1 is a line (1D Euclidean), \mathcal{M}_2 is embedded in 2D with curvature). Blue squares mark the marginal projections for x_1 and x_2 . The final generalized geodesic projection is the green diamond. The green diamond represents the length from the origin to the projected point on the product manifold (the projected point itself is not shown in the figure).

Proposition 2. *If $\int_{\mathbb{R}^d \times S_d^{++}(\mathbb{R})} c((\mu_1, \Sigma_1), (\mu_0, \Sigma_0))^p dG_1(\mu_1, \Sigma_1) < \infty$*

and $\int_{\mathbb{R}^d \times S_d^{++}(\mathbb{R})} c((\mu_0, \Sigma_0), (\mu_2, \Sigma_2))^p dG_2(\mu_2, \Sigma_2) < \infty$ for any $(\mu_0, \Sigma_0) \in \mathbb{R}^d \times S_d^{++}(\mathbb{R})$ with

$c((\mu_1, \Sigma_1), (\mu_2, \Sigma_2)) = \sqrt{\|\mu_1 - \mu_2\|_2^2 + \|\log \Sigma_1 - \log \Sigma_2\|_F^2}$, then $\text{Mix-SW}_p^p(G_1, G_2) < \infty$.

The proof of Proposition 2 is given in Appendix A.7. Next, we show that Mix-SW is a valid metric.

Theorem 1. *Mixed Sliced Wasserstein is a valid metric on the space of measures which belong to $\mathcal{P}(\mathbb{R}^d \times S_d^{++}(\mathbb{R}))$ and satisfy the constraint in Proposition 2.*

The proof of Theorem 1 is given in Appendix A.8 which extends the technique of the proofs in Bonnotte (2013), Nadjahi et al. (2020), and Bonet et al. (2023) with the usage of the generalized geodesic projection.

Corollary 1. *Mix-SW is also a metric on the space of finite mixture of Gaussians.*

Corollary 1 is based on the identifiability of finite mixture of Gaussians (Proposition 2 in Yakowitz and Spragins (1968)) and it suggests that Mix-SW can also be used to compare two finite mixtures of Gaussians based on their mixing measures on $\mathbb{R}^d \times S_d^{++}(\mathbb{R})$.

On the computational side, the expectation in Definition 2 is intractable. We therefore employ Monte Carlo estimation to approximate Mix-SW. Specifically, we sample $(w_1, v_1, A_1), \dots, (w_L, v_L, A_L) \stackrel{\text{i.i.d.}}{\sim} \mathcal{U}(\mathbb{S}) \otimes \mathcal{U}(\mathbb{S}^{d-1}) \otimes \mathcal{U}(S_d(\mathbb{R}))$. The Monte Carlo estimate of Mix-SW is then defined as:

$$\widehat{\text{Mix-SW}}_p^p(G_1, G_2) = \frac{1}{L} \sum_{l=1}^L W_p^p(P_{V_{w,l}} \# G_1, P_{V_{w,l}} \# G_2), \quad (14)$$

where $V_{w,l} = (w_{l1}v_l, w_{l2}A_l)$. When G_1 and G_2 are discrete measures with K_1 and K_2 supports, respectively, the time complexity of Mix-SW is $\mathcal{O}((K_1 + K_2 + L)d^3 + L(K_1 + K_2)d^2 + L(K_1 + K_2)\log(K_1 + K_2))$, which arises from sampling $A \sim \mathcal{U}(S_d(\mathbb{R}))$ (see Algorithm 1 in Bonet et al. (2023)), computing the matrix logarithm, projecting the samples, and solving one-dimensional Wasserstein distances. The projection complexity of Mix-SW is $\mathcal{O}(Ld^2)$ since it requires storing L projection matrices A_1, \dots, A_L . We present a pseudo algorithm for computing Mix-SW in Algorithm 3 in Appendix A.5.

3.3 Sliced Mixture Wasserstein

Mix-SW compares measures in $\mathcal{P}(\mathbb{R}^d \times S_d^{++}(\mathbb{R}))$. But it is not specifically designed for Gaussian mixing measures. To leverage the structure of Gaussian mixing measures, we introduce a variant called the sliced mixture Wasserstein (SMix-W) distance, which compares Gaussian mixing measures via their induced mixture of Gaussian measures. SMix-W is inspired by the Mixture Wasserstein distance (Delon and Desolneux, 2020), which is defined specifically for comparing mixtures of Gaussian measures. We refer the reader to Appendix A.4 for a more detail discussion of the connection to Mixture Wasserstein. We start with the linearity of mixture of Gaussians. When $G_1 = \sum_{i=1}^{K_1} \alpha_i \delta_{(\mu_{1i}, \Sigma_{1i})}$ and $G_2 = \sum_{j=1}^{K_2} \beta_j \delta_{(\mu_{2j}, \Sigma_{2j})}$,

we have $F_1 = f * G_1 := \sum_{i=1}^{K_1} \alpha_i \mathcal{N}(\mu_{1i}, \Sigma_{1i})$ and $F_2 = f * G_2 := \sum_{j=1}^{K_2} \beta_j \mathcal{N}(\mu_{2j}, \Sigma_{2j})$. For a vector $v \in \mathbb{R}^d$ and $P_v(x) = \langle x, v \rangle$, we have $P_v \# F_1 := \sum_{i=1}^{K_1} \alpha_i \mathcal{N}(\langle v, \mu_{1i} \rangle, v^\top \Sigma_{1i} v)$ and $P_v \# F_2 := \sum_{j=1}^{K_2} \beta_j \mathcal{N}(\langle v, \mu_{2j} \rangle, v^\top \Sigma_{2j} v)$, which are two one-dimensional Gaussian mixtures with the mixing measures $P_v \# G_1$ and $P_v \# G_2$ with $P_v(\mu, \Sigma) = (\langle v, \mu \rangle, v^\top \Sigma v)$. After applying linear projection to the mixture Gaussians (or P_v on the Gaussian mixing measure), we can use generalized geodesic projections to obtain the sliced Mixture Wasserstein as follows:

Definition 3. *Given two finite discrete measures G_1 and G_2 in $\mathcal{P}(\mathbb{R}^d \times S_d^{++}(\mathbb{R}))$, $p \geq 1$, and $P_{v,w}(\mu, \Sigma) = w_1 \langle v, \mu \rangle + w_2 \log(\sqrt{v^\top \Sigma v})$, the sliced mixture Wasserstein (SMix-W) is defined as follows:*

$$SMix-W_p^p(G_1, G_2) = \mathbb{E}_{(w,v) \sim \mathcal{U}(\mathbb{S}) \otimes \mathcal{U}(\mathbb{S}^{d-1})} [W_p^p(P_{v,w} \# G_1, P_{v,w} \# G_2)],$$

where $\mathcal{U}(\mathcal{X})$ is the uniform distribution over the set \mathcal{X} .

Compared to SW and Mix-SW, the projection space of SMix-W is smaller, specifically $\mathbb{S}^{d-1} \times \mathbb{S}$, as it utilizes a single projecting direction v for both μ and Σ .

Proposition 3. *If $\int_{\mathbb{R}^d \times S_d^{++}(\mathbb{R})} c((\mu_1, \Sigma_1), (\mu_0, \Sigma_0))^p dG_1(\mu_1, \Sigma_1) < \infty$ and $\int_{\mathbb{R}^d \times S_d^{++}(\mathbb{R})} c((\mu_0, \Sigma_0), (\mu_2, \Sigma_2))^p dG_2(\mu_2, \Sigma_2) < \infty$ for any $(\mu_0, \Sigma_0) \in \mathbb{R}^d \times S_d^{++}(\mathbb{R})$ with $c((\mu_1, \Sigma_1), (\mu_2, \Sigma_2)) = \sqrt{\|\mu_1 - \mu_2\|_2^2 + 0.25 \log(\lambda_{\max}(\Sigma_1, \Sigma_2))^2}$ ($\lambda_{\max}(\Sigma_1, \Sigma_2)$ is the largest eigenvalue of the generalized problem $\Sigma_1 v = \lambda \Sigma_2 v$), then $SMix-W_p^p(G_1, G_2) < \infty$.*

The proof of Proposition 3 is given in Appendix A.9. After showing the SMix-W is bounded, we show that SMix-W is a valid metric for discrete measures on $\mathcal{P}(\mathbb{R}^d \times S_d^{++}(\mathbb{R}))$.

Theorem 2. *SMix-W is a valid metric on the space of finite discrete measures on $\mathcal{P}(\mathbb{R}^d \times S_d^{++}(\mathbb{R}))$ which satisfy the constraint in Proposition 3.*

The proof of Theorem 2 is given in Appendix A.10. The claim is established only for finite discrete measures on $\mathcal{P}(\mathbb{R}^d \times S_d^{++}(\mathbb{R}))$ since the proof of identity of indiscernibles of

SMix-W relies on the identifiability of finite mixture of Gaussians (Proposition 2 in Yakowitz and Spragins (1968)). In addition, from the identifiability, SMix-W is also a metric between finite mixtures of Gaussians measures.

On the computational side, the expectation in Definition 3 is also intractable. As before, we use Monte Carlo estimation to approximate the value of SMix-W. In particular, we sample $(w_1, v_1), \dots, (w_L, v_L) \stackrel{i.i.d.}{\sim} \mathcal{U}(\mathbb{S}) \otimes \mathcal{U}(\mathbb{S}^{d-1})$. The Monte Carlo estimation of SMix-W is defined as follows:

$$\widehat{\text{SMix-W}}_p^p(G_1, G_2) = \frac{1}{L} \sum_{l=1}^L W_p^p(P_{v_l, w_l} \# G_1, P_{v_l, w_l} \# G_2). \quad (15)$$

When G_1 and G_2 are discrete measures with K_1 and K_2 supports, respectively, the time complexity of SMix-W is $\mathcal{O}(L(K_1 + K_2 + 2)d^2 + L(K_1 + K_2) \log(K_1 + K_2))$, due to the computation of the projections and the solving of one-dimensional Wasserstein distances. The projection complexity of SMix-W is $\mathcal{O}(Ld)$, as it only requires storing L projections of $(w_1, v_1), \dots, (w_L, v_L)$. We observe that SMix-W reduces the time complexity from $\mathcal{O}(d^3)$ of Mix-SW to $\mathcal{O}(d^2)$ by exploiting the linearity of mixtures of Gaussians. Compared to vectorized SW and Mix-SW with $\mathcal{O}(d^2)$ in projection complexity, SMix-W has a better projection complexity of $\mathcal{O}(d)$, making it more scalable with respect to the number of dimensions. Furthermore, a lower-dimensional projection space for SMix-W may lead to a reduced number of projections L required for a good approximation. We present a pseudo algorithm for computing SMix-W in Algorithm 4 in Appendix A.5.

4 Empirical Analysis

We assess clustering and density estimation under two alternative approaches to summarize the posterior Monte Carlo samples: summarizing random partitions versus the proposed novel method of summarizing random mixing measures. For the first approach, we utilize

the SALSO package (Dahl et al., 2022) with its greedy search algorithm to obtain point estimates of the random partition using Binder, VI , and omARI. Below we will refer to these summaries as the “alternative approaches”. For the proposed new methods, we employ vectorized SW, Mix-SW, and SMix-W (all are approximated with $L = 100$ projections) to obtain point estimates of the random mixing measures. For evaluation, we use Binder loss, VI loss, and omARI loss to assess clustering performance, while we employ approximated Total Variation (TV) and approximated SW (with $L = 1000$ projections) computed on a grid over the data space to evaluate the density estimates. Note that this setup favor approaches that use the same loss to summarize posterior Monte Carlo samples.

The proposed approach remains valid for any BNP mixture models with arbitrary prior and sampling models. For easier exposition and to facilitate the comparison we work with the conjugate truncated Dirichlet process mixture of Gaussians models (Ishwaran and James, 2001):

$$\beta_1, \dots, \beta_K \mid \alpha \sim \text{Beta}(1, \alpha), \quad w_k = \beta_k \prod_{j=1}^{k-1} (1 - \beta_j), \quad (16)$$

$$z_i \mid w_1, \dots, w_K \sim \text{Multinomial}(w_1, \dots, w_K), \quad (\mu_i, \Sigma_i) \mid \mu_0, \lambda, \Psi, \nu \sim \mathcal{NIW}(\mu_0, \lambda, \Psi, \nu),$$

$$y_i \mid \mu_{1:K}, \Sigma_{1:K}, z_i = k \sim \mathcal{N}(\mu_k, \Sigma_k), \quad i = 1, \dots, n,$$

where $K > 0$ is the truncation level, and \mathcal{NIW} denotes the Normal Inverse Wishart distribution. Inference under (16) of the above model can be carried out efficiently by a blocked Gibbs sampler (Ishwaran and James, 2001) to simulate from the joint distribution $p(\beta_{1:K}, \mu_{1:K}, \Sigma_{1:K}, z_{1:n} \mid y_{1:n})$. We implement inference in Python for a simulated dataset in Section 4.1, and for the Old Faithful geyser dataset (Azzalini and Bowman, 1990) in Section 4.2. In Appendix A.11, we report a brief sensitivity analysis for the Monte Carlo approximation of SW, Mix-SW, and SMix-W.

4.1 Simulated data

Let $V = 1.5^2 \cdot I_2$. We sample 200 i.i.d data

$$y_i \stackrel{\text{i.i.d.}}{\sim} \frac{1}{4}\mathcal{N}((-2, -2), V) + \frac{1}{4}\mathcal{N}((2, -2), V) + \frac{1}{4}\mathcal{N}((-2, 2), V) + \frac{1}{4}\mathcal{N}((2, 2), V),$$

$i = 1, \dots, n = 200$. We run 10000 blocked Gibbs sampler iterations (9000 burn-in iterations) with the following hyperparameters $\mu_0 = (0, 0)$, $\Psi = \text{diag}((1, 1))$, $\lambda = 1$, $\nu = 4$, $\alpha = 1$, $K = 100$. We repeat the simulation 25 times.

Figure 2 plots the simulated data, the true generating density, the true cluster arrangements, and the density and estimated clusters obtained under different loss functions in the two summarization approaches from the first simulation repetition. We evaluate the density on a 100×100 grid, with the range defined by $(\min y_i - 1, \max y_i + 1)$. For the first approach, starting with a point estimate of the partition, we first determine $\hat{\mathbf{z}}$ (using Binder, VI, or omARI loss), and then evaluate $\mathbb{E}[F \mid \hat{\mathbf{z}}, y_{1:n}]$ by using 10 more iterations of the MCMC simulation to update F (freezing $\hat{\mathbf{z}}$) i.e., we evaluate $\mathbb{E}[F(x) \mid \hat{\mathbf{z}}, y_{1:n}] \approx \frac{1}{10} \sum_{i=1}^{10} F_i(x)$ with $F_1, \dots, F_{10} \sim p(F \mid \hat{\mathbf{z}}, y_{1:n})$.

Table 1 reports the mean and the standard deviation of expected losses and the relative loss, relative to the simulation truth, using Binder, VI, and omARI, from 25 repeated simulations. The expected losses reflect the quality of the point estimate with respect to the posterior while the relative losses reflect the quality of the point estimate in the frequentist sense. We note that summarizing the random mixing measures yields comparable mean expected Binder, mean expected VI, and mean expected omARI loss compared to the alternative approach of summarizing the partition first despite the evaluation metric using the same losses. In particular, summarizing the random mixing measure always yields the second-best results for all clustering metrics. The proposed approach yields a smaller number of clusters than summarizing random partitions with Binder and omARI loss. All SW metrics behave similarly in terms of expected Binder and expected omARI loss. SW

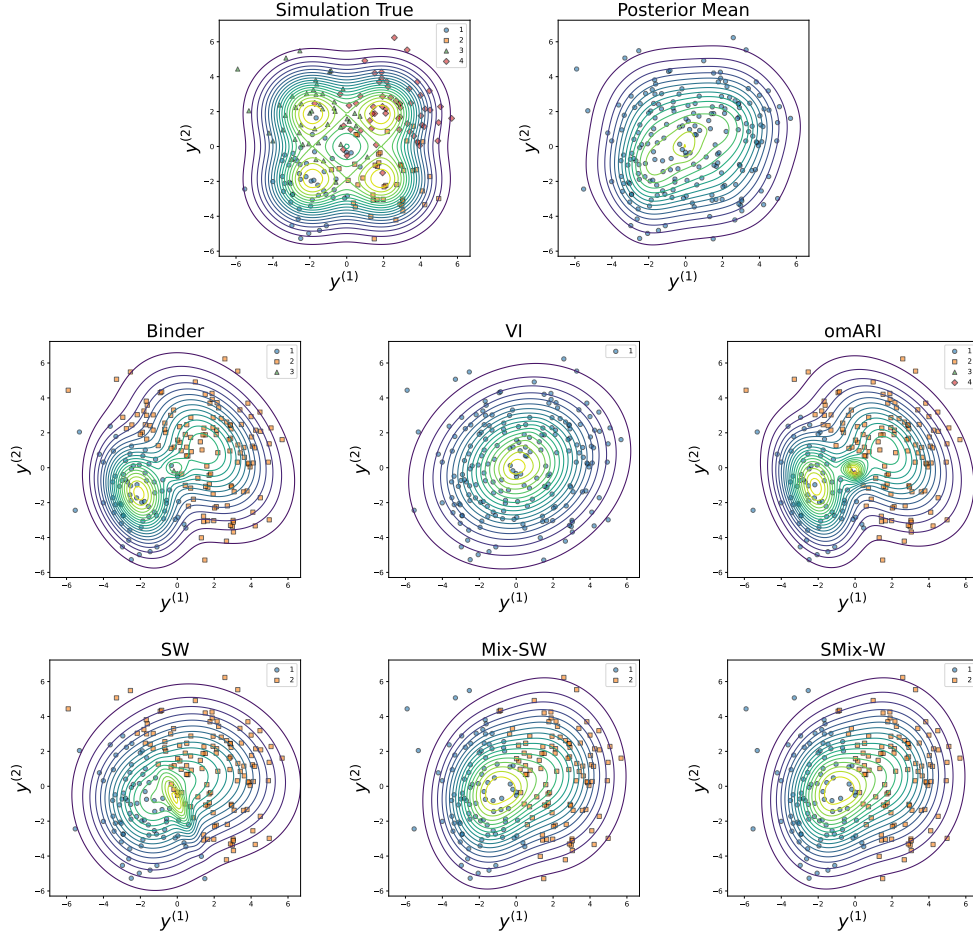


Figure 2: The figure shows the simulated data (dots), the true generating density (first plot, contours), the true cluster indices (first plot), the estimated density and cluster indices under different loss functions (other plots). For Binder, VI, and omARI loss, the estimated density is conditional on the partition. For SW, Mix-SW, and SMix-W, the contours show the estimated mixing measure and the Gaussian kernel.

yields a lower expected VI loss than Mix-SW and SMix-W. However, Mix-SW leads to the best relative Binder and relative VI while SMix-W yield the best relative omARI loss. We conclude that with respect to the reported point estimate $\hat{\mathbf{z}}$ the approaches that start with a point estimate of the random mixing measure perform comparable to approaches that start with the random partition. In addition, all SW variants seem to work similarly in terms of clustering performance.

Table 2 reports the means and the standard deviations of expected distances and relative distances, relative to the simulation truth using total variation distance and SW_2 distance. For the alternative approaches that first summarize the partitions (based on Binder, VI, or omARI loss), the losses are averaged over 10 Monte Carlo samples of F (freezing the point

	k_n^*	$\mathbb{E}[B(\hat{z}, z)]$	$B(\hat{z}, z^*)$	$\mathbb{E}[VI(\hat{z}, z)]$	$VI(\hat{z}, z^*)$	$\mathbb{E}[omARI(\hat{z}, z)]$	$omARI(\hat{z}, z^*)$
Binder	3.52 ± 3.08	0.1615 ± 0.0887	0.5103 ± 0.2112	0.7818 ± 0.4968	1.9904 ± 0.1501	0.6654 ± 0.2978	0.8213 ± 0.1672
VI	1.52 ± 0.59	0.1702 ± 0.1039	0.5495 ± 0.2119	0.6976 ± 0.4172	1.9216 ± 0.1343	0.7070 ± 0.3155	0.8442 ± 0.1721
omARI	5.76 ± 2.26	0.2170 ± 0.0970	0.4362 ± 0.1609	1.0043 ± 0.3267	2.0480 ± 0.2323	0.6065 ± 0.2385	0.7783 ± 0.1545
SW	1.76 ± 0.78	0.1651 ± 0.0909	0.5150 ± 0.2047	0.7474 ± 0.4558	1.9352 ± 0.1352	0.6687 ± 0.2944	0.8225 ± 0.1643
Mix-SW	1.84 ± 0.85	0.1661 ± 0.0920	0.5057 ± 0.2064	0.7684 ± 0.4764	1.9342 ± 0.1449	0.6657 ± 0.2912	0.8140 ± 0.1709
SMix-W	2.04 ± 1.02	0.1673 ± 0.0933	0.5021 ± 0.2067	0.7938 ± 0.4916	1.9616 ± 0.1416	0.6667 ± 0.2868	0.8134 ± 0.1701

Table 1: Simulated data: the table summarizes the estimated partitions under different loss functions. The columns from left to right are the number of unique clusters, expected Binder loss, relative Binder loss, expected VI loss, relative VI loss, expected omARI loss, and relative omARI loss. Lower losses are better.

	$\mathbb{E}[TV(\hat{F}, F)]$	$TV(\hat{F}, F^*)$	$\mathbb{E}[SW_2(\hat{F}, F)]$	$SW_2(\hat{F}, F^*)$
Binder	0.2363 ± 0.0639	0.4262 ± 0.0281	0.2845 ± 0.0201	0.5807 ± 0.0898
VI	0.2267 ± 0.0516	0.4140 ± 0.0291	0.2858 ± 0.0196	0.5742 ± 0.1034
omARI	0.2650 ± 0.0566	0.4392 ± 0.0303	0.2950 ± 0.0235	0.5777 ± 0.0955
SW	0.1947 ± 0.0569	0.4032 ± 0.0424	0.2424 ± 0.0384	0.5695 ± 0.1238
Mix-SW	0.1907 ± 0.0533	0.4019 ± 0.0368	0.2318 ± 0.0283	0.5614 ± 0.1116
SMix-W	0.1955 ± 0.0556	0.4060 ± 0.0282	0.2282 ± 0.0262	0.5600 ± 0.1008

Table 2: Simulated data: the table summarizes the estimated density under different loss functions. Columns from left to right are expected Total Variation distance, Total Variation to the true density, expected SW_2 distance, and SW_2 distance to the true density. Lower distances are better.

	$\mathbb{E}[SW_2(\hat{G}, G)]$	$SW_2(\hat{G}, G^*)$	$\mathbb{E}[\text{Mix-SW}_2(\hat{G}, G)]$	$\text{Mix-SW}_2(\hat{G}, G^*)$	$\mathbb{E}[\text{SMix-W}_2(\hat{G}, G)]$	$\text{SMix-W}_2(\hat{G}, G^*)$
SW	0.8492 ± 0.1881	1.9826 ± 0.5224	0.5315 ± 0.1553	1.2406 ± 0.2891	0.4591 ± 0.1600	1.1762 ± 0.2701
Mix-SW	0.8882 ± 0.2027	2.0051 ± 0.4975	0.5183 ± 0.1528	1.2278 ± 0.2893	0.4446 ± 0.1574	1.1648 ± 0.2694
SMix-W	0.8991 ± 0.2128	2.0283 ± 0.5401	0.5264 ± 0.1567	1.2254 ± 0.2950	0.4410 ± 0.1563	1.1574 ± 0.2740

Table 3: Simulated data: evaluation of point estimates of the mixing measures G under SW, Mix-SW, and SMix-W. The columns from left to right are expected SW_2 distance, SW_2 distance to the simulation true G^* , expected Mix- SW_2 distance, Mix- SW_2 distance G^* , expected SMix- W_2 distance, and SMix- W_2 distance to G^* . Lower distances are better.

estimate \hat{z}) as discussed. Naturally, the proposed approach of summarizing the mixing measures first results in lower losses. Among SW variants, Mix-SW leads to the best total variation distances (both expected distance and relative distance). SMix-W leads to the best point estimate of the density in terms of both expected SW and relative SW distance.

Table 3 reports the means and the standard deviations of expected losses and relative losses, relative to the simulation truth, using SW_2 distance, Mix- SW_2 distance, and SMix- W_2 distance from 25 repeat simulations. Not surprisingly, inference under each distance performs best when used for its intended evaluation.

For summaries based on 1000 posterior MCMC samples of the mixing measures (truncation level $K = 100$), SW and SMix-W take about 10 minutes while Mix-SW takes about 40 minutes on a Nvidia GeForce RTX 3060 with Pytorch implementation. Summarizing random partition with the SALSO package (R implementation), takes about 2 minutes for 1000 MCMC posterior samples of 200 cluster indices using any of the three losses (Binder, VI, omARI). The reason that summarizing mixing measure is slower is that the mixing measure contains more information than the cluster indices. The computation of summarizing the mixing measure depends on the truncation level K , the dimension d , but does not depend on the number of data points n . In contrast, summarizing the partition depends only on n . Therefore, with a very large n , summarizing the mixing measure might be more efficient. Once the point estimate of the mixing measure is evaluated, it takes only 1 minutes to obtain the point estimate of the random partition and the density. In contrast, it takes around 5 minutes to evaluate the density estimate with 10 more MCMC iterations starting from an estimated partition.

4.2 Old Faithful Geyser dataset

The Old Faithful geyser dataset contains 272 data samples in 2 dimensions. We run 10000 blocked Gibbs sampler iterations (9000 burn-in iterations) with the following hyperparameters $\mu_0 = (3, 70)$, $\Psi = \text{diag}((4, 26))$, $\lambda = 1$, $\nu = 4$, $\alpha = 1$, $K = 100$. Figure 3 shows the data, along with the density estimate and estimated partition obtained under different loss functions using the two approaches.

Table 4 reports the expected losses using Binder loss, VI, and omARI loss. We note a similar overall pattern as in the simulation: summarizing the random mixing measures yields comparable expected Binder loss and expected omARI loss compared to partition-focused approaches. In particular, summarizing the random mixing measures with SW, Mix-SW, and SMix-W results in only about a 3.38% increase in expected Binder loss com-

	k_n^*	$\mathbb{E}[B(\hat{z}, z)]$	$\mathbb{E}[VI(\hat{z}, z)]$	$\mathbb{E}[omARI(\hat{z}, z)]$
Binder	8	0.0296	0.2588	0.0594
VI	3	0.0333	0.2446	0.0667
omARI	8	0.0296	0.2588	0.0594
SW	4	0.0303	0.2602	0.0607
Mix-SW	3	0.0306	0.2678	0.0614
SMix-W	3	0.0306	0.2678	0.0614

Table 4: Old Faithful: same as corresponding columns in Table 1.

	$\mathbb{E}[TV(\hat{F}, F)]$	$\mathbb{E}[SW_2(\hat{F}, F)]$
Binder	0.2128	1.0558
VI	0.2102	1.0293
omARI	0.2128	1.0558
SW	0.1901	0.8671
Mix-SW	0.1852	0.7759
SMix-W	0.1852	0.7752

Table 5: Old Faithful: same as Table 2 (columns 1 and 3).

pared to the best expected Binder loss, and only about a 3.37% increase in expected omARI loss compared to the best expected omARI loss. For VI loss, the proposed approach results in an increase of about 8.86% in expected VI loss compared to the best expected VI loss. Table 5 reports the expected losses using total variation and SW_2 distance for the density estimation. For the partition-focused approaches (using Binder, VI, or omARI loss), the losses are averaged over 10 Monte Carlo samples of F , as under the previously described simulation study. Summarizing the mixing measure naturally leads to better density estimates than summarizing partitions first. In particular, the best partition-focused method reports a 13.5% higher expected total variation loss and 19.23% higher expected SW loss compared to Mix-SW and SMix-W. Furthermore, we find that SMix-W and Mix-SW compare favorably to SW.

Finally, in Table 6 we report the expected losses under SW_2 distance, Mix- SW_2 distance, and SMix- W_2 distance for estimating the mixing measure. Again we observe similar patterns as in the simulation study. Inference under each loss function performs best when used for its intended evaluation.

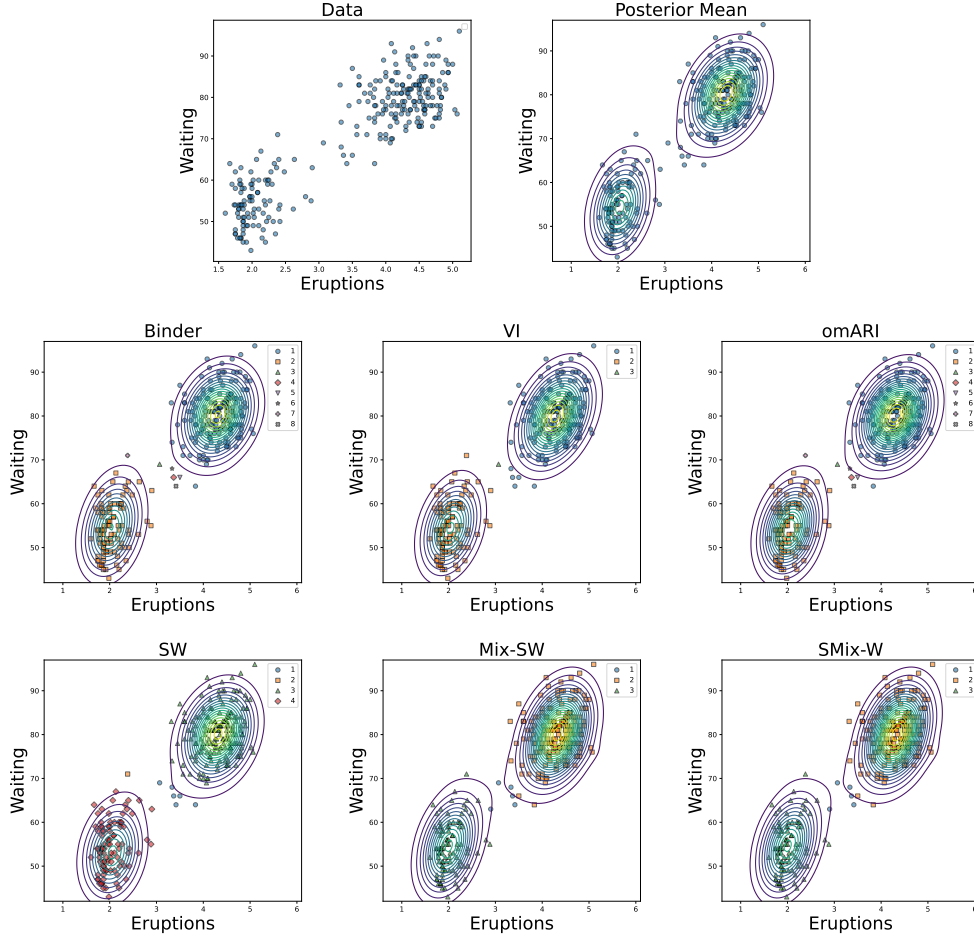


Figure 3: Old Faithful: same as Figure 2.

	$\mathbb{E}[SW_2(\hat{G}, G)]$	$\mathbb{E}[\text{Mix-SW}_2(\hat{G}, G)]$	$\mathbb{E}[\text{SMix-W}_2(\hat{G}, G)]$
SW	3.1228	1.4876	1.4831
Mix-SW	3.7931	1.3186	1.3091
SMix-W	3.7917	1.3186	1.3091

Table 6: Old Faithful: same as corresponding columns in Table 3.

5 Conclusion

We present a new approach for summarizing posterior inference under Bayesian Nonparametric (BNP) mixture models. The main difference to commonly used methods is that we start with a summary of the mixing measures. Our method minimizes the posterior expected loss using a discrepancy between measures, utilizing the computationally scalable SW distance. For Gaussian mixture models, we introduce two variants: mixed sliced Wasserstein (Mix-SW) and sliced mixture Wasserstein (SMix-W). Mix-SW uses general-

ized geodesic projection on the product of the Euclidean manifold and the manifold of symmetric positive definite matrices, providing a principled meaningful metric for comparing Gaussian mixing measures. SMix-W leverages the linearity of Gaussian mixtures for efficient projection. Empirical analyses show that our summarization approach yields more accurate density estimates while maintaining a good partition summary.

Limitations of the proposed approach include the potential suboptimality of the reported point estimate of the mixing measures, as the solution is limited to the available posterior Monte Carlo samples. In addition, the conventional sliced Wasserstein distance might not be optimal for all mixture models; therefore, different variants should be designed to exploit specific geometry, as we do for Gaussian mixtures.

The proposed framework addresses the problem of summarizing posterior inference on a random partition when it is being used, leaving the judgement about appropriate use of the chosen model to the investigators. In particular, it has been observed that clustering of high-dimensional data might be challenging (Chandra et al., 2023).

SUPPLEMENTARY MATERIALS

The Supplementary Materials include Appendices and codes to reproduce empirical parts of the paper.

Appendices: Appendices are in the file “appendix.pdf” which contains technical proofs and additional discussion.

Python code, R code, and data: The file “code.zip” contains Python code, R code, and data to reproduce all empirical parts of the paper. We refer the reader to the “README.md” file inside the zip archive for detailed instructions.

References

- Ali, S. M. and Silvey, S. D. (1966), “A general class of coefficients of divergence of one distribution from another,” *Journal of the Royal Statistical Society: Series B (Methodological)*, 28, 131–142.
- Azzalini, A. and Bowman, A. W. (1990), “A look at some data on the Old Faithful geyser,” *Journal of the Royal Statistical Society: Series C (Applied Statistics)*, 39, 357–365.
- Baringhaus, L. and Franz, C. (2004), “On a new multivariate two-sample test,” *Journal of Multivariate Analysis*, 88, 190–206.
- (2010), “Rigid motion invariant two-sample tests,” *Statistica Sinica*, 1333–1361.
- Binder, D. A. (1978), “Bayesian cluster analysis,” *Biometrika*, 65, 31–38.
- Boedihardjo, M. T. (2025), “Sharp bounds for max-sliced Wasserstein distances,” *Foundations of Computational Mathematics*, 1–32.
- Bonet, C., Drumetz, L., and Courty, N. (2025), “Sliced-Wasserstein distances and flows on Cartan-Hadamard manifolds,” *Journal of Machine Learning Research*, 26, 1–76.

- Bonet, C., Malézieux, B., Rakotomamonjy, A., Drumetz, L., Moreau, T., Kowalski, M., and Courty, N. (2023), “Sliced-Wasserstein on symmetric positive definite matrices for M/EEG signals,” in *International Conference on Machine Learning*, PMLR.
- Bonneel, N., Rabin, J., Peyré, G., and Pfister, H. (2015), “Sliced and Radon Wasserstein Barycenters of Measures,” *Journal of Mathematical Imaging and Vision*, 1, 22–45.
- Bonnotte, N. (2013), *Unidimensional and evolution methods for optimal transportation*, Ph.D. thesis, Paris 11.
- Chandra, N. K., Canale, A., and Dunson, D. B. (2023), “Escaping the curse of dimensionality in bayesian model-based clustering,” *Journal of Machine Learning Research*, 24, 1–42.
- Cuturi, M. (2013), “Sinkhorn distances: Lightspeed computation of optimal transport,” in *Advances in Neural Information Processing Systems*.
- Dahl, D. B., Johnson, D. J., and Müller, P. (2022), “Search algorithms and loss functions for Bayesian clustering,” *Journal of Computational and Graphical Statistics*, 31, 1189–1201.
- Delon, J. and Desolneux, A. (2020), “A Wasserstein-type distance in the space of Gaussian mixture models,” *SIAM Journal on Imaging Sciences*, 13, 936–970.
- Feydy, J., Séjourné, T., Vialard, F.-X., Amari, S.-i., Trounev, A., and Peyré, G. (2019), “Interpolating between Optimal Transport and MMD using Sinkhorn Divergences,” in *The 22nd International Conference on Artificial Intelligence and Statistics*.
- Ghosal, S. and van der Vaart, A. W. (2017), *Fundamentals of nonparametric Bayesian inference*, volume 44, Cambridge University Press.
- Griffin, J. E. (2016), “An adaptive truncation method for inference in Bayesian nonparametric models,” *Statistics and Computing*, 26, 423–441.

- Gu, A., Sala, F., Gunel, B., and Ré, C. (2019), “Learning mixed-curvature representations in products of model spaces,” in *International Conference on Learning Representations*, volume 5.
- Ishwaran, H. and James, L. F. (2001), “Gibbs sampling methods for stick-breaking priors,” *Journal of the American Statistical Association*, 96, 161–173.
- Kalli, M., Griffin, J. E., and Walker, S. G. (2011), “Slice sampling mixture models,” *Statistics and Computing*, 21, 93–105.
- Lau, J. W. and Green, P. J. (2007), “Bayesian model-based clustering procedures,” *Journal of Computational and Graphical Statistics*, 16, 526–558.
- Leluc, R., Dieuleveut, A., Portier, F., Segers, J., and Zhuman, A. (2024), “Sliced-Wasserstein estimation with spherical harmonics as control variates,” in *International Conference on Machine Learning*.
- MacEachern, S. N. (1999), “Dependent Nonparametric Processes,” in *ASA Proceedings of the Section on Bayesian Statistical Science, Alexandria, VA: American Statistical Association..*
- Meilă, M. (2007), “Comparing clusterings—an information based distance,” *Journal of Multivariate Analysis*, 98, 873–895.
- Nadjahi, K., Durmus, A., Chizat, L., Kolouri, S., Shahrampour, S., and Simsekli, U. (2020), “Statistical and topological properties of sliced probability divergences,” *Advances in Neural Information Processing Systems*, 33, 20802–20812.
- Neal, R. M. (2000), “Markov chain sampling methods for Dirichlet process mixture models,” *Journal of Computational and Graphical Statistics*, 9, 249–265.
- Nguyen, K., Bariletto, N., and Ho, N. (2024), “Quasi-Monte Carlo for 3D Sliced Wasserstein,” in *International Conference on Learning Representations*.

- Nguyen, K. and Ho, N. (2023), “Sliced Wasserstein Estimator with Control Variates,” *International Conference on Learning Representations*.
- (2024), “Hierarchical Hybrid Sliced Wasserstein: A Scalable Metric for Heterogeneous Joint Distributions,” *Advances in Neural Information Processing Systems*, 108140–108166.
- Nguyen, K., Ho, N., Pham, T., and Bui, H. (2021), “Distributional Sliced-Wasserstein and Applications to Generative Modeling,” in *International Conference on Learning Representations*.
- Nguyen, V., Epps, J., and Bailey, J. (2010), “Information theoretic measures for clusterings comparison: variants, properties, normalization and correction for chance,” *Journal of Machine Learning Research*, 11, 2837–2854.
- Paty, F.-P. and Cuturi, M. (2019), “Subspace robust Wasserstein distances,” in *International Conference on Machine Learning*, PMLR.
- Pennec, X., Sommer, S., and Fletcher, T. (2019), *Riemannian geometric statistics in medical image analysis*, Academic Press.
- Peyré, G., Cuturi, M., et al. (2019), “Computational optimal transport: With applications to data science,” *Foundations and Trends® in Machine Learning*, 11, 355–607.
- Quintana, F. A., Müller, P., Jara, A., and MacEachern, S. N. (2022), “The dependent Dirichlet process and related models,” *Statistical Science*, 37, 24–41.
- Rabin, J., Peyré, G., Delon, J., and Bernot, M. (2012), “Wasserstein barycenter and its application to texture mixing,” in *Scale Space and Variational Methods in Computer Vision: Third International Conference, SSVM 2011, Ein-Gedi, Israel, May 29–June 2, 2011, Revised Selected Papers 3*, Springer.

- Rand, W. M. (1971), “Objective criteria for the evaluation of clustering methods,” *Journal of the American Statistical Association*, 66, 846–850.
- Rastelli, R. and Friel, N. (2018), “Optimal Bayesian estimators for latent variable cluster models,” *Statistics and Computing*, 28, 1169–1186.
- Villani, C. (2009), *Optimal transport: old and new*, volume 338, Springer.
- Wade, S. and Ghahramani, Z. (2018), “Bayesian Cluster Analysis: Point Estimation and Credible Balls (with Discussion),” *Bayesian Analysis*, 13, 559–626.
- Yakowitz, S. J. and Spragins, J. D. (1968), “On the identifiability of finite mixtures,” *The Annals of Mathematical Statistics*, 39, 209–214.

A Appendices

A.1 Acronyms

We summarize the a list of acronyms used in the paper as follow:

- BNP: Bayesian Nonparametric.
- SW: sliced Wasserstein.
- Mix-SW: mixed sliced Wasserstein.
- SMix-W: sliced mixture Wasserstein.
- MAP: maximum a posteriori.
- MCMC: Markov chain Monte Carlo.
- VI: variational information.
- omARI: one minus adjusted Rand index.

A.2 Review on Riemannian Manifolds

A Riemannian manifold (\mathcal{M}, G) of dimension d is a space that behaves locally as a linear space diffeomorphic to \mathbb{R}^d , named a tangent space. For any $x \in \mathcal{M}$, the associated tangent space is defined as $T_x\mathcal{M}$ which supports an inner product $\langle \cdot, \cdot \rangle_x : T_x\mathcal{M} \times T_x\mathcal{M} \rightarrow \mathbb{R}$ i.e., $\langle u, v \rangle_x = u^\top G(x)v$. The joint space of the manifold and the tangent space is called the tangent bundle $T\mathcal{M} = \{x \in \mathcal{M}, v \in T_x\mathcal{M}\}$.

Geodesics. Given two points $x, y \in \mathcal{M}$, the smooth curve $\gamma : [0, 1] \rightarrow \mathcal{M}$ such as $\gamma(0) = x, \gamma(1) = y$ is called geodesic if it minimizes the length:

$$\mathcal{L}(\gamma) = \int_0^1 \sqrt{\langle \gamma'(t), \gamma'(t) \rangle_{\gamma(t)}} dt,$$

where $\gamma'(t)$ is the derivative of the curve $\gamma(t)$ with respect to t , which belongs to the tangent space $T_{\gamma(t)}\mathcal{M}$ for any $t \in [0, 1]$. The length of the geodesic line is the geodesic distance.

$$c(x, y) = \inf_{\gamma | \gamma(0)=x, \gamma(1)=y} \mathcal{L}(\gamma).$$

Exponential Map. Let $x \in \mathcal{M}$, for any $v \in T_x\mathcal{M}$, there exists a unique geodesic γ with $\gamma(0) = x$ and $\gamma'(0) = v$, denoted as $\gamma_{x,v}$. The exponential map $\exp : T\mathcal{M} \rightarrow \mathcal{M}$ maps $v \in T_x\mathcal{M}$ back to the manifold at the point reached by the geodesic $\gamma(1)$. In particular, we have the following definition of the exponential map:

$$\forall (x, v) \in T\mathcal{M}, \exp_x(v) = \gamma_{x,v}(1)$$

A.3 Mixed Sliced Wasserstein

Geodesic Projection Let γ be a curve on the manifold \mathcal{M} , and denote \mathcal{A} as the set of all points belonging to that curve. The projection of a point $x \in \mathcal{M}$ onto the curve γ is defined as: $\tilde{P}_\gamma(x) = \arg \min_{y \in \mathcal{A}} c(x, y)$, where c is a geodesic distance. If we constrain γ to be a curve that passes through the origin (denoted as o) with unit velocity v (i.e., $\langle v, v \rangle_o = 1$), then we have $\Gamma = \{\exp_o(tv) \mid t \in \mathbb{R}\}$, where $\exp_o(\cdot)$ is the exponential map at the origin. The coordinates of the projection can be determined by solving:

$$P_{\gamma(o,v)}(x) := P_v(x) = \arg \min_{t \in \mathbb{R}} c(x, \exp_o(tv)). \quad (17)$$

Product Manifold of $\mathbb{R}^d \times S_d^{++}(\mathbb{R})$. From Pennec et al. (2019), the origin of $S_d^{++}(\mathbb{R})$ is the identity matrix I , and the tangent space is the space of all symmetric matrices. The exponential map is given by $\exp_I(A) = \exp(A) = \sum_{n=0}^{\infty} \frac{A^n}{n!}$. While there are multiple geodesic distances on $S_d^{++}(\mathbb{R})$, we focus on the Log-Euclidean metric defined as:

$c_{LE}(\Sigma_1, \Sigma_2) = \|\log \Sigma_1 - \log \Sigma_2\|_F$, where $\log X = A$ if $\exp(A) = X$. Since X is a symmetric positive definite matrix, we can use spectral decomposition: $X = Q\Lambda Q^T$, which gives us $\log X = Q \text{diag}(\log \lambda_1, \dots, \log \lambda_d) Q^T$. The origin of the manifold $\mathbb{R}^d \times S_d^{++}(\mathbb{R})$ is $o = (0, I)$, where 0 is the d -dimensional zero vector. The exponential map in this manifold is defined as $\exp_o((\mu, \Sigma)) = (\mu, \exp(\Sigma))$. A geodesic distance of the product manifolds is defined as follows (Gu et al., 2019): $c((\mu_1, \Sigma_1), (\mu_2, \Sigma_2)) = \sqrt{\|\mu_1 - \mu_2\|_2^2 + c_{LE}(\Sigma_1, \Sigma_2)^2}$.

A.4 Sliced Mixture Wasserstein

Mixture Wasserstein distance. Given two discrete measures G_1 and G_2 belonging to $\mathcal{P}(\mathbb{R}^d \times S_d^{++}(\mathbb{R}))$, and a Gaussian kernel $f(x \mid \mu, \Sigma)$, we define F_1 and F_2 as the corresponding mixtures of Gaussian measures, i.e., $F_1 = f * G_1$ and $F_2 = f * G_2$, where $*$ denotes the standard convolution operation. The Mixture Wasserstein (MW) distance (Delon and Desolneux, 2020) is defined as:

$$\text{MW}_2^2(F_1, F_2) = \inf_{\pi \in \Pi(F_1, F_2) \cap \text{GMM}_{2d}(\infty)} \int_{\mathbb{R}^d \times \mathbb{R}^d} \|x - y\|_2^2 d\pi(x, y), \quad (18)$$

where $\text{GMM}_{2d}(\infty)$ denotes the set of all finite Gaussian mixture distributions in $2d$ dimensions. Compared to Wasserstein distance, Mixture Wasserstein consider only couplings that are finite Gaussian mixtures. When $G_1 = \sum_{i=1}^{K_1} \alpha_i \delta_{(\mu_{1i}, \Sigma_{1i})}$ and $G_2 = \sum_{j=1}^{K_2} \beta_j \delta_{(\mu_{2j}, \Sigma_{2j})}$, the Mixture Wasserstein distance simplifies to: $\min_{\eta \in \Gamma(\alpha, \beta)} \sum_{i=1}^{K_1} \sum_{j=1}^{K_2} \eta_{ij} W_2^2(\mathcal{N}(\mu_{1i}, \Sigma_{1i}), \mathcal{N}(\mu_{2j}, \Sigma_{2j}))$. Using the closed-form expression of the Wasserstein-2 distance between two Gaussian distributions, we can rewrite this as:

$$\min_{\eta \in \Gamma(\alpha, \beta)} \sum_{i=1}^{K_1} \sum_{j=1}^{K_2} \eta_{ij} \left(\|\mu_{1i} - \mu_{2j}\|_2^2 + \text{Tr}(\Sigma_{1i}) + \text{Tr}(\Sigma_{2j}) - \text{Tr} \left((\Sigma_{1i}^{1/2} \Sigma_{2j} \Sigma_{1i}^{1/2})^{1/2} \right) \right).$$

One-dimensional Mixture Wasserstein distance. In preparation of the upcoming definition of sliced MW by comparing one-dimensional projections of mixtures of normals,

we note the special case of one-dimensional MW distance. When $G_1 = \sum_{i=1}^{K_1} \alpha_i \delta_{(\mu_{1i}, \sigma_{1i}^2)}$ and $G_2 = \sum_{j=1}^{K_2} \beta_j \delta_{(\mu_{2j}, \sigma_{2j}^2)}$ are one-dimensional mixtures of Gaussians, we have:

$$\begin{aligned} \text{MW}_2^2(F_1, F_2) &= \min_{\gamma \in \Gamma(\alpha, \beta)} \sum_{i=1}^{K_1} \sum_{j=1}^{K_2} \gamma_{i,j} ((\mu_{1i} - \mu_{2j})^2 + (\sigma_{1i} - \sigma_{2j})^2) \\ &= W_2^2((\text{Id}, \sqrt{\cdot})\#G_1, (\text{Id}, \sqrt{\cdot})\#G_2), \quad (19) \end{aligned}$$

which implies that the Mixture Wasserstein distance between one-dimensional Gaussian mixtures behaves like a two-dimensional Wasserstein-2 distance on the mixing measures, with a square root scaling applied to the variances. It is important to note that the one-dimensional MW distance does not offer computational advantages, as it is not equivalent to a one-dimensional Wasserstein distance.

Sliced Mixture Wasserstein. After applying linear projection to the mixture Gaussians (or P'_v on the Gaussian mixing measure), we can use one-dimensional MW in (19) to compare them i.e.,

$$\mathbb{E}_{v \sim \mathcal{U}(\mathbb{S}^{d-1})} [\text{MW}_2^2(P_v\#F_1, P_v\#F_2)] = \mathbb{E}_{v \sim \mathcal{U}(\mathbb{S}^{d-1})} [W_2^2((\text{Id}, \sqrt{\cdot})\#P'_v\#G_1, (\text{Id}, \sqrt{\cdot})\#P'_v\#G_2)]. \quad (20)$$

However, MW does not have a closed-form expression, as discussed. Since MW is equivalent to the Wasserstein-2 distance between mixing measures, we can replace it with the SW distance to achieve computational benefits, as SW is equivalent to the Wasserstein distance under a mild assumption (Bonnotte, 2013) i.e., atoms of two measures belong to a ball of size $R > 0$. This replacement leads to a novel variant of SW distance for mixtures of Gaussians and their mixing measures.

We can rewrite SMix-W in Definition 3 as:

$$\text{SMix-}W_2^2(G_1, G_2) = \mathbb{E}_{v \sim \mathcal{U}(\mathbb{S}^{d-1})} \left[SW_2^2 \left((\text{Id}, \log \circ \sqrt{\cdot})\#P'_v\#G_1, (\text{Id}, \log \circ \sqrt{\cdot})\#P'_v\#G_2 \right) \right]$$

Algorithm 1 Summarizing the posterior of mixing measure

Input: Posterior samples of the mixing measure G_1, \dots, G_M ($M \geq 2$), and discrepancy \mathcal{D} (assumed to be symmetric).
Initialize $C \in \mathbb{R}^{M \times M}$
for $i = 1$ to M **do**
 for $j = i + 1$ to M **do**
 $C_{ij} = C_{ji} = \mathcal{D}(G_i, G_j)$
 end for
end for
Find $i^* = \arg \min_{i \in \{1, \dots, M\}} \sum_{j=1}^M C_{ij}$
Return: G_{i^*} .

Algorithm 2 Computational algorithm of vectorized sliced Wasserstein

Input: Probability measures $G_1 = \sum_{i=1}^{K_1} \alpha_i \delta_{(\mu_{1i}, \Sigma_{1i})}$ and $G_2 = \sum_{j=1}^{K_2} \beta_j \delta_{(\mu_{2j}, \Sigma_{2j})}$, $p \geq 1$, function $V(\theta)$, and the number of projections L .
Vectorize $V\#G_1 = \sum_{i=1}^{K_1} \alpha_i \delta_{V(\mu_{1i}, \Sigma_{1i})}$ and $V\#G_2 = \sum_{j=1}^{K_2} \beta_j \delta_{V(\mu_{2j}, \Sigma_{2j})}$
for $l = 1$ to L **do**
 Sample $v_l \sim \mathcal{U}(\mathbb{S}^{d(d+1)-1})$
 Compute $P_{v_l}\#V\#G_1 = \sum_{i=1}^{K_1} \alpha_i \delta_{v_l^\top V(\mu_{1i}, \Sigma_{1i})}$ and $v_l\#V\#G_2 = \sum_{j=1}^{K_2} \beta_j \delta_{v_l^\top V(\mu_{2j}, \Sigma_{2j})}$
 Compute $W_p^p(P_{v_l}\#V\#G_1, P_{v_l}\#V\#G_2)$ as in (8).
end for
Return: $\widehat{SW}_p(G_1, G_2; L) = \left(\frac{1}{L} \sum_{l=1}^L W_p^p(P_{v_l}\#V\#G_1, P_{v_l}\#V\#G_2) \right)^{\frac{1}{p}}$.

which replaces MW of the mixtures in (20) with the SW of the mixing measures, incorporating a logarithmic transformation to adjust the standard deviation as a geodesic projection. Compared to SW and Mix-SW, the projection space of SMix-W is smaller, specifically $\mathbb{S}^{d-1} \times \mathbb{S}$, as it utilizes a single projecting direction v for both the mean μ and the covariance matrix Σ .

A.5 Algorithms

We present the pseudo algorithm for the proposed posterior summarization framework in Algorithm 1. Moreover, we also give pseudo algorithms for vectorized SW, Mix-SW, and SMix-W in Algorithm 2, Algorithm 3, and Algorithm 4 in turn.

Algorithm 3 Computational algorithm of mixed sliced Wasserstein (Mix-SW)

Input: Probability measures $G_1 = \sum_{i=1}^{K_1} \alpha_i \delta_{(\mu_{1i}, \Sigma_{1i})}$ and $G_2 = \sum_{j=1}^{K_2} \beta_j \delta_{(\mu_{2j}, \Sigma_{2j})}$, $p \geq 1$, and the number of projections L .

for $l = 1$ to L **do**

Sample $v_l \sim \mathcal{U}(\mathbb{S}^{d-1})$, $A_l \sim \mathcal{U}(S_d(\mathbb{R}))$, $w_l \sim \mathcal{U}(\mathbb{S})$.

Set $V_{w,l} = (w_l, v_l, A_l)$.

Compute $P_{V_{w,l}} \# G_1 = \sum_{i=1}^{K_1} \alpha_i \delta_{P_{V_{w,l}}(\mu_{1i}, \Sigma_{1i})}$ and $P_{V_{w,l}} \# G_2 = \sum_{j=1}^{K_2} \beta_j \delta_{P_{V_{w,l}}(\mu_{2j}, \Sigma_{2j})}$ as in (1).

Compute $W_p^p(P_{V_{w,l}} \# G_1, P_{V_{w,l}} \# G_2)$ as in (8).

end for

Return: $\widehat{\text{Mix-SW}}_p(G_1, G_2) = \left(\frac{1}{L} \sum_{l=1}^L W_p^p(P_{V_{w,l}} \# G_1, P_{V_{w,l}} \# G_2) \right)^{\frac{1}{p}}.$

Algorithm 4 Computational algorithm of sliced mixture Wasserstein (SMix-W)

Input: Probability measures $G_1 = \sum_{i=1}^{K_1} \alpha_i \delta_{(\mu_{1i}, \Sigma_{1i})}$ and $G_2 = \sum_{j=1}^{K_2} \beta_j \delta_{(\mu_{2j}, \Sigma_{2j})}$, $p \geq 1$, and the number of projections L .

for $l = 1$ to L **do**

Sample $v_l \sim \mathcal{U}(\mathbb{S}^{d-1})$, $w_l \sim \mathcal{U}(\mathbb{S})$.

Compute $P_{v_l, w_l} \# G_1 = \sum_{i=1}^{K_1} \alpha_i \delta_{P_{v_l, w_l}(\mu_{1i}, \Sigma_{1i})}$ and $P_{v_l, w_l} \# G_2 = \sum_{j=1}^{K_2} \beta_j \delta_{P_{v_l, w_l}(\mu_{2j}, \Sigma_{2j})}$ as in (1).

Compute $W_p^p(P_{v_l, w_l} \# G_1, P_{v_l, w_l} \# G_2)$ as in (8).

end for

Return: $\widehat{\text{SMix-W}}_p(G_1, G_2) = \left(\frac{1}{L} \sum_{l=1}^L W_p^p(P_{v_l, w_l} \# G_1, P_{v_l, w_l} \# G_2) \right)^{\frac{1}{p}}.$

A.6 Proof of Proposition 1

By Definition 1, we have:

$$\begin{aligned} P_{V_w}((\mu, \Sigma)) &= \arg \min_{t \in \mathbb{R}} c(x, \exp_0(tV_w)) = \arg \min_{t \in \mathbb{R}} c^2(x, \exp_0(tV_w)) \\ &= \arg \min_{t \in \mathbb{R}} \|\mu - tw_1v\|_2^2 + \|\log \Sigma - \log \exp(tw_2A)\|_F \\ &= \arg \min_{t \in \mathbb{R}} \|\mu - tw_1v\|_2^2 + \|\log \Sigma - tw_2A\|_F \\ &= \arg \min_{t \in \mathbb{R}} \|\mu\|_2^2 + w_1^2 t^2 - 2w_1 t \langle \mu, v \rangle + w_2^2 t^2 + \text{Trace}((\log \Sigma)^2) - 2w_2 t \text{Trace}(A \log \Sigma) \\ &= \arg \min_{t \in \mathbb{R}} \|\mu\|_2^2 + t^2 - 2w_1 t \langle \mu, v \rangle + \text{Trace}((\log \Sigma)^2) - 2w_2 t \text{Trace}(A \log \Sigma) \\ &:= \arg \min_{t \in \mathbb{R}} f(t) \end{aligned}$$

Taking the derivative $\frac{d}{dt}f(t) = 2t - 2w_1\langle\mu, v\rangle - 2w_2\text{Trace}(A\log\Sigma)$, then set it to 0. We obtain: $P_{V_w}(\theta) = t^* = w_1\langle\mu, v\rangle + w_2\text{Trace}(A\log\Sigma)$, which completes the proof.

A.7 Proof of Proposition 2

Since $P_{V_w}((\mu, \Sigma)) = w_1\langle\mu, v\rangle + w_2\text{Trace}(A\log\Sigma)$ is a Borel measurable, using Lemma 6 in (Paty and Cuturi, 2019), we have:

$$\begin{aligned} W_p^p(P_{V_w}\sharp G_1, P_{V_w}\sharp G_2) &= \inf_{\pi_{V_w} \in \Pi(P_{V_w}\sharp G_1, P_{V_w}\sharp G_2)} \int_{\mathbb{R} \times \mathbb{R}} |x - y|^p d\pi_{V_w}(x, y) \\ &= \inf_{\pi \in \Pi(G_1, G_2)} \int_{\mathbb{R}^d \times S_d^{++}(\mathbb{R}) \times \mathbb{R}^d \times S_d^{++}(\mathbb{R})} |P_{V_w}(\mu_1, \Sigma_1) - P_{V_w}(\mu_2, \Sigma_2)|^p d\pi((\mu_1, \Sigma_1), (\mu_2, \Sigma_2)) \\ &\leq \inf_{\pi \in \Pi(G_1, G_2)} \int_{\mathbb{R}^d \times S_d^{++}(\mathbb{R}) \times \mathbb{R}^d \times S_d^{++}(\mathbb{R})} (|P_{V_w}(\mu_1, \Sigma_1) - P_{V_w}(\mu_0, \Sigma_0)| \\ &\quad + |P_{V_w}(\mu_0, \Sigma_0) - P_{V_w}(\mu_2, \Sigma_2)|)^p d\pi((\mu_1, \Sigma_1), (\mu_2, \Sigma_2)), \end{aligned}$$

where the inequality is due to the triangle inequality of the \mathbb{L}_1 norm. Using the Minkowski's inequality, we have:

$$\begin{aligned} W_p^p(P_{V_w}\sharp G_1, P_{V_w}\sharp G_2) &\leq \inf_{\pi \in \Pi(G_1, G_2)} \int_{\mathbb{R}^d \times S_d^{++}(\mathbb{R}) \times \mathbb{R}^d \times S_d^{++}(\mathbb{R})} 2^{p-1} (|P_{V_w}(\mu_1, \Sigma_1) - P_{V_w}(\mu_0, \Sigma_0)|^p \\ &\quad + |P_{V_w}(\mu_0, \Sigma_0) - P_{V_w}(\mu_2, \Sigma_2)|^p) d\pi_{V_w} d\pi((\mu_1, \Sigma_1), (\mu_2, \Sigma_2)) \\ &= 2^{p-1} \left(\int_{\mathbb{R}^d \times S_d^{++}(\mathbb{R})} |P_{V_w}(\mu_1, \Sigma_1) - P_{V_w}(\mu_0, \Sigma_0)|^p dG_1(\mu_1, \Sigma_1) \right. \\ &\quad \left. + \int_{\mathbb{R}^d \times S_d^{++}(\mathbb{R})} |P_{V_w}(\mu_0, \Sigma_0) - P_{V_w}(\mu_2, \Sigma_2)|^p dG_2(\mu_2, \Sigma_2) \right). \end{aligned}$$

Moreover, from the Cauchy–Schwarz’s inequality, we have:

$$\begin{aligned}
& |P_{V_w}(\mu_1, \Sigma_1) - P_{V_w}(\mu_0, \Sigma_0)| \\
&= |w_1 \langle \mu_1, v \rangle + w_2 \text{Trace}(A \log \Sigma_1) - w_1 \langle \mu_0, v \rangle - w_2 \text{Trace}(A \log \Sigma_0)| \\
&= |w_1 \langle \mu_1 - \mu_0, v \rangle + w_2 (\text{Trace}(A \log \Sigma_1) - \text{Trace}(A \log \Sigma_0))| \\
&\leq \sqrt{w_1^2 + w_2^2} \sqrt{\langle \mu_1 - \mu_0, v \rangle^2 + (\text{Trace}(A(\log \Sigma_1 - \log \Sigma_0)))^2} \\
&= \sqrt{\langle \mu_1 - \mu_0, v \rangle^2 + (\text{Trace}(A(\log \Sigma_1 - \log \Sigma_0)))^2} \\
&\leq \sqrt{\|v\|_2^2 \|\mu_1 - \mu_0\|_2^2 + \|A\|_F^2 \|\log \Sigma_1 - \log \Sigma_0\|_F^2} \\
&= \sqrt{\|\mu_1 - \mu_0\|_2^2 + \|\log \Sigma_1 - \log \Sigma_0\|_F^2} = c((\mu_1, \Sigma_1), (\mu_0, \Sigma_0)).
\end{aligned}$$

From the assumption, we get:

$$\begin{aligned}
W_p^p(P_{V_w} \# G_1, P_{V_w} \# G_2) &\leq 2^{p-1} \left(\int_{\mathbb{R}^d \times S_d^{++}(\mathbb{R})} c((\mu_1, \Sigma_1), (\mu_0, \Sigma_0))^p dG_1(\mu_1, \Sigma_1) \right. \\
&\quad \left. + \int_{\mathbb{R}^d \times S_d^{++}(\mathbb{R})} c((\mu_0, \Sigma_0), (\mu_2, \Sigma_2))^p dG_2(\mu_2, \Sigma_2) \right) < \infty,
\end{aligned}$$

which completes the proof.

A.8 Proof of Theorem 1

Symmetry and Non-negativity. The symmetry and non-negativity of Mix-SW follows directly the symmetry and non-negativity of the Wasserstein distance (Peyré et al., 2019) since it is the expectation of projected Wasserstein distance.

Triangle Inequality. Let consider three measure G_1, G_2, G_3 , using the triangle inequality of Wasserstein distance, we have:

$$\begin{aligned} \text{Mix-SW}_p(G_1, G_2) &= \left(\mathbb{E}_{(w,v,A) \sim \mathcal{U}(\mathbb{S}) \otimes \mathcal{U}(\mathbb{S}^{d-1}) \otimes \mathcal{U}(S_d(\mathbb{R}))} [W_p^p(P_{V_w} \# G_1, P_{V_w} \# G_2)] \right)^{\frac{1}{p}} \\ &\leq \left(\mathbb{E}_{(w,v,A) \sim \mathcal{U}(\mathbb{S}) \otimes \mathcal{U}(\mathbb{S}^{d-1}) \otimes \mathcal{U}(S_d(\mathbb{R}))} [(W_p(P_{V_w} \# G_1, P_{V_w} \# G_3) + W_p(P_{V_w} \# G_3, P_{V_w} \# G_2))^p] \right)^{\frac{1}{p}}. \end{aligned}$$

Using the Minkowski's inequality, we get:

$$\begin{aligned} \text{Mix-SW}_p(G_1, G_2) &\leq \left(\mathbb{E}_{(w,v,A) \sim \mathcal{U}(\mathbb{S}) \otimes \mathcal{U}(\mathbb{S}^{d-1}) \otimes \mathcal{U}(S_d(\mathbb{R}))} [W_p^p(P_{V_w} \# G_1, P_{V_w} \# G_3)] \right)^{\frac{1}{p}} \\ &\quad + \left(\mathbb{E}_{(w,v,A) \sim \mathcal{U}(\mathbb{S}) \otimes \mathcal{U}(\mathbb{S}^{d-1}) \otimes \mathcal{U}(S_d(\mathbb{R}))} [W_p^p(P_{V_w} \# G_3, P_{V_w} \# G_2)] \right)^{\frac{1}{p}} \\ &= \text{Mix-SW}_p(G_1, G_3) + \text{Mix-SW}_p(G_3, G_2), \end{aligned}$$

which completes the proof of triangle inequality.

Identity of indiscernibles. When $G_1 = G_2$, we have directly $\text{Mix-SW}_p^p(G_1, G_2) = 0$.

We now prove that if $\text{Mix-SW}_p^p(G_1, G_2) = 0$, we get $G_1 = G_2$. We first rewrite $P_{V_w}(\mu, \Sigma)$ as a composition of two function i.e., $P_{V_w}(\mu, \Sigma) = P_w \circ P_V(\mu, \Sigma)$. In particular, $P_V : \mathbb{R}^d \times S_d^{++}(\mathbb{R}) \rightarrow \mathbb{R}^2$ i.e., $P_V(\mu, \Sigma) = (\langle \mu, v \rangle, \text{Trace}(A \log \Sigma))$ ($V = (v, A)$) and $P_w : \mathbb{R}^2 \rightarrow \mathbb{R}$ i.e., $P_w(x) = \langle w, x \rangle$. We then can rewrite mixed Sliced Wasserstein distance as:

$$\begin{aligned} \text{Mix-SW}_p^p(G_1, G_2) &= \mathbb{E}_{(w,v,A) \sim \mathcal{U}(\mathbb{S}) \otimes \mathcal{U}(\mathbb{S}^{d-1}) \otimes \mathcal{U}(S_d(\mathbb{R}))} [W_p^p(P_{V_w} \# G_1, P_{V_w} \# G_2)] \\ &= \mathbb{E}_{(v,A) \sim \mathcal{U}(\mathbb{S}^{d-1}) \otimes \mathcal{U}(S_d(\mathbb{R}))} [\mathbb{E}_{w \sim \mathcal{U}(\mathbb{S})} [W_p^p(P_w \# P_V \# G_1, P_w \# P_V \# G_2)]] \\ &= \mathbb{E}_{(v,A) \sim \mathcal{U}(\mathbb{S}^{d-1}) \otimes \mathcal{U}(S_d(\mathbb{R}))} [SW_p^p(P_V \# G_1, P_V \# G_2)]. \end{aligned}$$

When $\text{Mix-SW}_p^p(G_1, G_2) = 0$, it means that $SW_p^p(P_V \# G_1, P_V \# G_2) = 0$ for $\mathcal{U}(\mathbb{S}^{d-1}) \otimes \mathcal{U}(S_d(\mathbb{R}))$ -almost every (v, A) . Using the identity of indiscernibles property of SW (Bonnotte, 2013), we have $P_V \# G_1 = P_V \# G_2$ for $\mathcal{U}(\mathbb{S}^{d-1}) \otimes \mathcal{U}(S_d(\mathbb{R}))$ -almost every (v, A) . Let

denote $\mathcal{F}[P_V \# G_1]$ and $\mathcal{F}[P_V \# G_2]$ as the Fourier transform of G_1 and G_2 respectively, we have $\mathcal{F}[P_V \# G_1] = \mathcal{F}[P_V \# G_2]$ for $\mathcal{U}(\mathbb{S}^{d-1}) \otimes \mathcal{U}(S_d(\mathbb{R}))$ -almost every (v, A) . Moreover, for all $y \in \mathbb{R}^2$, we have:

$$\begin{aligned}
\mathcal{F}[P_V \# G_1](y) &= \int_{\mathbb{R}^2} e^{-2i\pi \langle y, x \rangle} d(P_V \# G_1)(x) \\
&= \int_{\mathbb{R}^d \times S_d^{++}(\mathbb{R})} e^{-2i\pi (y_1 \langle v, \mu_1 \rangle + y_2 \langle A, \log \Sigma_1 \rangle_F)} dG_1(\mu_1, \Sigma_1) \\
&= \int_{\mathbb{R}^d \times S_d^{++}(\mathbb{R})} e^{-2i\pi (\langle y_1 v, \mu_1 \rangle + \langle y_2 A, \log \Sigma_1 \rangle_F)} dG_1(\mu_1, \Sigma_1) \\
&= \int_{\mathbb{R}^d \times S_d^{++}(\mathbb{R})} e^{-2i\pi (\langle y_1 v, \mu_1 \rangle + \langle y_2 A, S_1 \rangle_F)} d((Id, \log) \# G_1)(\mu_1, S_1) \\
&= \mathcal{F}[(Id, \log) \# G_1](y_1 v, y_2 A).
\end{aligned}$$

Therefore, we obtain $\mathcal{F}[(Id, \log) \# G_1](y_1 v, y_2 A) = \mathcal{F}[(Id, \log) \# G_2](y_1 v, y_2 A)$ for $\mathcal{U}(\mathbb{S}^{d-1}) \otimes \mathcal{U}(S_d(\mathbb{R}))$ -almost every (v, A) . By injectivity of the Fourier transform, we get $(Id, \log) \# G_1 = (Id, \log) \# G_2$. Since the function $f(\mu, \Sigma) = (\mu, \log \Sigma)$ is injective i.e., $f^{-1}(\mu, \Sigma) = (\mu, \exp(\Sigma))$, we obtain $G_1 = G_2$, which completes the proof.

A.9 Proof of Proposition 3

Since $P_{v,w}(\mu, \Sigma) = w_1 \langle v, \mu \rangle + w_2 \log(\sqrt{v^\top \Sigma v})$ is a Borel measurable, using Lemma 6 in (Paty and Cuturi, 2019), we have:

$$\begin{aligned}
W_p^p(P_{v,w} \# G_1, P_{v,w} \# G_2) &= \inf_{\pi_{v,w} \in \Pi(P_{v,w} \# G_1, P_{v,w} \# G_2)} \int_{\mathbb{R} \times \mathbb{R}} |x - y|^p d\pi_{v,w}(x, y) \\
&= \inf_{\pi \in \Pi(G_1, G_2)} \int_{\mathbb{R}^d \times S_d^{++}(\mathbb{R}) \times \mathbb{R}^d \times S_d^{++}(\mathbb{R})} |P_{v,w}(\mu_1, \Sigma_1) - P_{v,w}(\mu_2, \Sigma_2)|^p d\pi((\mu_1, \Sigma_1), (\mu_2, \Sigma_2)).
\end{aligned}$$

Using the Minkowski's inequality, we have:

$$\begin{aligned}
W_p^p(P_{v,w} \# G_1, P_{v,w} \# G_2) &\leq \inf_{\pi \in \Pi(G_1, G_2)} \int_{\mathbb{R}^d \times S_d^{++}(\mathbb{R}) \times \mathbb{R}^d \times S_d^{++}(\mathbb{R})} 2^{p-1} (|P_{v,w}(\mu_1, \Sigma_1) - P_{v,w}(\mu_0, \Sigma_0)|^p \\
&\quad + |P_{v,w}(\mu_0, \Sigma_0) - P_{v,w}(\mu_2, \Sigma_2)|^p) d\pi_{V_w} d\pi((\mu_1, \Sigma_1), (\mu_2, \Sigma_2)) \\
&= 2^{p-1} \left(\int_{\mathbb{R}^d \times S_d^{++}(\mathbb{R})} |P_{v,w}(\mu_1, \Sigma_1) - P_{v,w}(\mu_0, \Sigma_0)|^p dG_1(\mu_1, \Sigma_1) \right. \\
&\quad \left. + \int_{\mathbb{R}^d \times S_d^{++}(\mathbb{R})} |P_{v,w}(\mu_0, \Sigma_0) - P_{v,w}(\mu_2, \Sigma_2)|^p dG_2(\mu_2, \Sigma_2) \right).
\end{aligned}$$

Moreover, from the Cauchy-Schwarz's inequality, we have:

$$\begin{aligned}
&|P_{v,w}(\mu_1, \Sigma_1) - P_{v,w}(\mu_0, \Sigma_0)| \\
&= |w_1 \langle v, \mu_1 \rangle + w_2 \log(\sqrt{v^\top \Sigma_1 v}) - w_1 \langle v, \mu_0 \rangle + w_2 \log(\sqrt{v^\top \Sigma_0 v})| \\
&= \left| w_1 \langle \mu_1 - \mu_0, v \rangle + 0.5w_2 \log \left(\frac{v^\top \Sigma_1 v}{v^\top \Sigma_0 v} \right) \right| \\
&\leq \sqrt{w_1^2 + w_2^2} \sqrt{\langle \mu_1 - \mu_0, v \rangle^2 + 0.25 \log \left(\frac{v^\top \Sigma_1 v}{v^\top \Sigma_0 v} \right)^2} \\
&= \sqrt{\langle \mu_1 - \mu_0, v \rangle^2 + 0.25 \log \left(\frac{v^\top \Sigma_1 v}{v^\top \Sigma_0 v} \right)^2} \\
&\leq \sqrt{\|v\|_2^2 \|\mu_1 - \mu_0\|_2^2 + 0.25 \log \left(\max_v \frac{v^\top \Sigma_1 v}{v^\top \Sigma_0 v} \right)^2} \\
&= \sqrt{\|\mu_1 - \mu_0\|_2^2 + 0.25 \log(\lambda_{\max}(\Sigma_1, \Sigma_2))^2} = c((\mu_1, \Sigma_0), (\mu_0, \Sigma_0)),
\end{aligned}$$

where $\lambda_{\max}(\Sigma_1, \Sigma_0)$ is the largest eigenvalue of the generalized problem $\Sigma_1 v = \lambda \Sigma_0 v$. From the assumption, we get:

$$\begin{aligned}
W_p^p(P_{v,w} \# G_1, P_{v,w} \# G_2) &\leq 2^{p-1} \left(\int_{\mathbb{R}^d \times S_d^{++}(\mathbb{R})} c((\mu_1, \Sigma_1), (\mu_0, \Sigma_0))^p dG_1(\mu_1, \Sigma_1) \right. \\
&\quad \left. + \int_{\mathbb{R}^d \times S_d^{++}(\mathbb{R})} c((\mu_0, \Sigma_0), (\mu_2, \Sigma_2))^p dG_2(\mu_2, \Sigma_2) \right) < \infty,
\end{aligned}$$

which completes the proof.

A.10 Proof of Theorem 2

Symmetry, Non-negativity, and Triangle Inequality. The symmetry, non-negativity, and triangle inequality of SMix-W can be obtained by following the proof for Mix-SW in Appendix A.8. In this section, we focus on the proof of identity of indiscernibles for SMix-W.

Identity of indiscernibles. When $G_1 = G_2$, we have directly $\text{SMix-}W_p^p(G_1, G_2) = 0$. We now prove that if $\text{SMix-}W_p^p(G_1, G_2) = 0$, we get $G_1 = G_2$. From the definition of SMix-W in Definition 3, we have:

$$\begin{aligned}\text{SMix-}W_p^p(G_1, G_2) &= \mathbb{E}_{(w,v) \sim \mathcal{U}(\mathbb{S}) \otimes \mathcal{U}(\mathbb{S}^{d-1})} [W_p^p(P_{v,w} \# G_1, P_{v,w} \# G_2)] \\ &= \mathbb{E}_{v \sim \mathcal{U}(\mathbb{S}^{d-1})} [SW_p^p((Id, \log \circ \sqrt{\cdot}) \# P'_v \# G_1, (Id, \log \circ \sqrt{\cdot}) \# P'_v \# G_2)].\end{aligned}$$

When $\text{SMix-}W_p^p(G_1, G_2) = 0$, it implies $SW_p^p((Id, \log \circ \sqrt{\cdot}) \# P'_v \# G_1, (Id, \log \circ \sqrt{\cdot}) \# P'_v \# G_2) = 0$ for $\mathcal{U}(\mathbb{S}^{d-1})$ -almost every v . Since $\log(x)$ is an injective function, it leads to the fact that $SW_p^p((Id, \sqrt{\cdot}) \# P'_v \# G_1, (Id, \sqrt{\cdot}) \# P'_v \# G_2) = 0$ for $\mathcal{U}(\mathbb{S}^{d-1})$ -almost every v . By the identity of indiscernibles of SW (Bonnotte, 2013), we have $(Id, \sqrt{\cdot}) \# P'_v \# G_1 = (Id, \sqrt{\cdot}) \# P'_v \# G_2$ for $\mathcal{U}(\mathbb{S}^{d-1})$ -almost every v with $P'_v(\mu, \Sigma) = (\langle v, \mu \rangle, v^\top \Sigma v)$. Since the square root function also injective on \mathbb{R}^+ , we have $P'_v \# G_1 = P'_v \# G_2$ which is equivalent to $P_v \# F_1 = P_v \# F_2$ for $\mathcal{U}(\mathbb{S}^{d-1})$ -almost every v with $P_v(x) = \langle v, x \rangle$ and $F_1 = f * G_1$ and $F_2 = f * G_2$ (f is the Gaussian density kernel). Let denote $\mathcal{F}[P_v \# F_1]$ and $\mathcal{F}[P_v \# F_2]$ as the Fourier transform of F_1 and F_2 respectively, we have $\mathcal{F}[P_v \# F_1] = \mathcal{F}[P_v \# F_2]$ for $\mathcal{U}(\mathbb{S}^{d-1})$ -almost every v . Moreover, for all

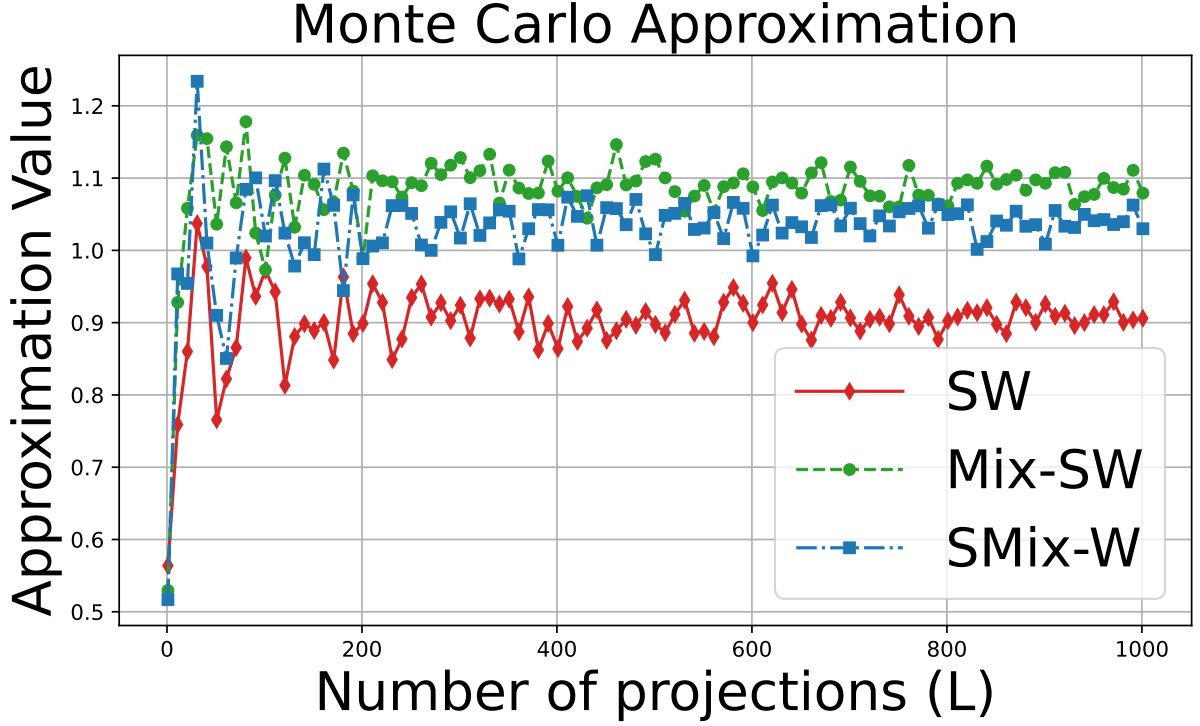


Figure 4: The figure show the approximation value of SW, Mix-SW, and SMix-W when increasing the number of projections L (the number of Monte Carlo samples).

$t \in \mathbb{R}$, we have:

$$\begin{aligned}\mathcal{F}[P_v \# F_1](t) &= \int_{\mathbb{R}^2} e^{-2i\pi t \epsilon} d(P_v \# F_1)(\epsilon) = \int_{\mathbb{R}^d} e^{-2i\pi t \langle v, x \rangle} dF_1(x) \\ &= \int_{\mathbb{R}^d} e^{-2i\pi \langle tv, x \rangle} dF_1(x) = \mathcal{F}[F_1](tv).\end{aligned}$$

Therefore, we get $\mathcal{F}[F_1](tv) = \mathcal{F}[F_2](tv)$ for $\mathcal{U}(\mathbb{S}^{d-1})$ -almost every v . By the injectivity of Fourier Transform, we get $F_1 = F_2$ which leads to $G_1 = G_2$ due to the identifiability of finite mixture of Gaussians (Proposition 2 in (Yakowitz and Spragins, 1968)), which concludes the proof.

A.11 Monte Carlo Approximation

We investigate the Monte Carlo approximation of SW, Mix-SW, and SMix-W when increasing the number of projections L (the number of Monte Carlo samples) in Figure 4. In

particular, we compare the mixing measures of the following two mixtures of Gaussians.

$$F_1(x) = 0.3 \cdot \mathcal{N} \left(x; \begin{bmatrix} 0 \\ 0 \end{bmatrix}, \begin{bmatrix} 1.0 & 0.8 \\ 0.8 & 1.5 \end{bmatrix} \right) + 0.4 \cdot \mathcal{N} \left(x; \begin{bmatrix} 3 \\ 3 \end{bmatrix}, \begin{bmatrix} 0.7 & -0.3 \\ -0.3 & 0.9 \end{bmatrix} \right) \\ + 0.3 \cdot \mathcal{N} \left(x; \begin{bmatrix} -3 \\ 3 \end{bmatrix}, \begin{bmatrix} 2.0 & 1.0 \\ 1.0 & 3.0 \end{bmatrix} \right),$$

and

$$F_2(x) = 0.2 \cdot \mathcal{N} \left(x; \begin{bmatrix} 1 \\ 1 \end{bmatrix}, \begin{bmatrix} 1.2 & 0.5 \\ 0.5 & 0.8 \end{bmatrix} \right) + 0.5 \cdot \mathcal{N} \left(x; \begin{bmatrix} 4 \\ 4 \end{bmatrix}, \begin{bmatrix} 0.4 & -0.2 \\ -0.2 & 0.6 \end{bmatrix} \right) \\ + 0.3 \cdot \mathcal{N} \left(x; \begin{bmatrix} -2 \\ 2 \end{bmatrix}, \begin{bmatrix} 1.5 & 0.7 \\ 0.7 & 2.5 \end{bmatrix} \right).$$

We vary the number of projections (Monte Carlo samples) from 1 to 1001 with step size 10. From Figure 4, we see that the approximation values of SW, Mix-SW, and SMix-W converges well when increasing L . We observe that $L = 100$ seems to give a good enough approximation for 2D mixtures of Gaussians. It is worth noting that we can adapt recent approaches such as control variates (Nguyen and Ho, 2023; Leluc et al., 2024) and quasi Monte Carlo (Nguyen et al., 2024) to improve the standard convergence rate of Monte Carlo i.e., $\mathcal{O}(L^{-1/2})$. However, we believe that adapting such techniques is worth for a careful investigation. Therefore, we leave it to future works.